A Dissertation

For the Degree of Doctor of Philosophy

Studies on Early Development of Primordial Germ Cells and Their Repopulation Capacity in Chicken

조류 생식세포의 초기 발달 및 복원 능력 연구

February, 2014

By

Hyung Chul Lee

Department of Agricultural Biotechnology

Graduate School, Seoul National University

Studies on Early Development of Primordial Germ Cells and Their Repopulation Capacity in Chicken

조류 생식세포의 초기 발달 및 복원 능력 연구

지도교수 한 재 용

이 논문을 농학박사 학위논문으로 제출함

2014년 2월
서울대학교 대학원
농생명공학부 동물유전공학 전공
이 형 철

이형철의 농학박사 학위논문을 인준함
2014년 2월

위 원 장 _____ (인)

부위원장 _____ (인)

위 원 _____ (인)

위 원 _____ (인)

위 원 _____ (인)

SUMMARY

Germ cells are the only population to transfer genetic and epigenetic information across generations. Studying their origin and characteristics is one of important topics in developmental and evolutionary biology. Among various species, the origin and specification of germ cells in birds have not been clearly defined. Besides, information about cleavage stages, the period that the developmental processes start and germ cells may arise, is insufficient, so that comprehensive studies are needed. Also, the research on the restorable proliferation of primordial germ cells (PGCs) in the gonads that can contribute to understand regenerative medicine is not studied, so far. In the present study, we analyzed the developmental dynamics of intrauterine embryo development in chicken and studied the origin of germ cells by tracing the expression of germ cell-specific genes. Also, we investigated the compensatory proliferation of PGCs in the gonads after busulfan treatment.

The first study was undertaken to elucidate detailed event of early embryogenesis in chicken embryos using a noninvasive egg retrieval technique before oviposition. White Leghorn intrauterine eggs were retrieved from hens and morphogenetic observation was made under both bright field and fluorescent image in a time course manner. Differing from mammals, asymmetric cleavage to yield preblastodermal cells was observed throughout early embryogenesis. The first two divisions occurred synchronously and four polarized preblastodermal cells resulted after cruciform cleavage. Then, asynchronous cleavage continued in a radial manner and overall cell size in the initial cleavage region was smaller than that in the distal area. Numerous sperms were visible, regardless of zygotic nuclei formation. Condensed sperm heads were present mainly in the perivitelline space and cytoplasm, and rarely in the yolk region, while decondensed sperm heads

were only visible in the yolk. In conclusion, apparent differences in sperm dynamics and early cleavage events compared with mammalian embryos were detected in chick embryo development, which demonstrated polarized cleavage with penetrating supernumerary sperm into multiple regions.

Based on the information of intrauterine chick embryos, we investigated origin of germ cells in chicken. We found that *cDAZL* mRNA was expressed specifically in germ cells throughout all stages of development in company with our previous study. During oocyte-to-zygote transition, *cDAZL* mRNA was localized in the perinuclear region of oocyte and the central region of zygote as a granule. In the EM study of zygote, electron-dense granules with numerous mitochondria were observed During intrauterine embryo development, cDAZL gene showed kinetics of expression pattern; localization in cleavage furrows during initial cleavages (EGK.I-III), subcellular localization in presumptive primordial germ cells (pPGCs) during cleavage progression (EGK.IV-VI) and finally diffused in the cytoplasm of PGCs during late intrauterine stages (EGK.VI-X) that indicated primordial germ cells (PGCs) may first arise at least from EGK.VI. cDAZL and CVH protein was also co-localized in cleavage furrows and PGCs. In addition, PGCs which were found at EGK.VI-X were located not only in the most upper layer (future epiblast) but also in the lower layers (future hypoblast) that indicated chicken PGCs were already present not only in the epiblast but also in the hypoblast in pre-streak stage embryos. Phosphorylation of RNA polymerase II in PGCs was synchronized with other somatic cells that indicated global transcriptional repression in PGCs during specification is not a common mechanism in chicken. Taken together, these results suggest that the germ plasm in chicken are consistently located in the center of embryo during specification, and PGCs are distinguished from somatic cells by germline-specific transcription at EGK.VI-VII.

Little is known about the cellular responses of PGCs after treatment with toxic chemicals such as busulfan during embryo development. Thus, we investigated the elimination, restorative ability, and cell cycle status of endogenous chicken PGCs after busulfan treatment. Busulfan was emulsified in sesame oil by a dispersion-emulsifying system and injected into the chick blastoderm (embryonic stage X). Subsequently, we conducted flow cytometry analysis to evaluate changes in the PGC population and cell cycle status, and immunohistochemistry to examine the germ cell proliferation. Results of flow cytometry and immunohistochemistry analyses after busulfan treatment showed that the proportion of male PGCs at embryonic day 9 and female PGCs at embryonic day 7 were increased by approximately 60% when compared to embryonic day 5.5, indicating the existence of a compensatory mechanism in PGCs in response to the cytotoxic effects of busulfan. Results of cell cycling analysis showed that the germ cells in G0/G1 phase were significantly decreased, while S/G2/M-phase germ cells were significantly increased in the treatment group compared to the untreated control group in both 9-day-old male and female embryos. In addition, in the proliferation analysis with 5-ethynyl-2′-deoxyuridine (EdU) incorporation, we found that the proportion of EdU positive cells among VASA (VASA homolog) positive cells in the 9-day embryonic gonads of busulfan treated group was significantly higher than control group. We conclude that PGCs enter a restoration pathway by promoting their cell cycle after experiencing a cytotoxic effect.

Through our results, intrauterine embryo development and cleavage progression of chicken are different from those of mammals. To know the mechanisms of cleavage progression, lineage specification and polarity formation, gene-expression patterns and functional studies should be done in the future. Also, studying of the biological function for polyspermy will contribute to understanding of the unique developmental characteristics in chicken. Germ cells

seem to be specified by the “predetermined” mode in chicken. However, whether signaling pathways and zygotic genome activation (ZGA) are related to specification or not should be identified through further studies for clarify this. Also, in the future, it should be identified what mechanisms regulate the reconstitution of PGC population after busufan treatment. Taken together, our results in the present study will contribute to understanding for developmental dynamics of early chick embryo and germ cells, and potency of primordial germ cells.

Keywords: chicken, intrauterine embryos, cleavage, polyspermy, primordial germ cells, proliferation, busulfan, pluripotency

Student Number: 2008-21375

CONTENTS

LIST OF FIGURES

CHAPTER 3

CHAPTER 4

CHAPTER 5

LIST OF TABLES

CHAPTER 3

CHAPTER 4

CHAPTER 5

LIST OF ABBREVIATIONS

Blimp1	B-lymphocyte-induced maturation protein 1
BSA	Bovine serum albumin
CVH	Chicken vasa homologue
DAPI	4',6-diamidino-2-phenylindole
DAZL	Deleted in azoospermia-like
DIG	Digoxigenin
EDTA	ethylenediaminetetraacetic acid
EG&K or EGK	Eyal-Giladi and Kochav
EGCs	Embryonic germ cells
ESCs	Embryonic stem cell
FITC	fluorescein isothiocyanate
GLM	General linear model
GSCs	Germline stem cells
GV	Germinal vesicle
MBT	Mid-blastrular transition
Mvh	Mouse vasa homolog
MZT	Maternal-to-zygotic transition
PAS	Periodic acid Schiff
PBS	Phosphate-buffered saline
pgc	Polar granule component
PGCs	primordial germ cells

PGPR90	Polyglycerol polyricinoleate
PI	Propidium iodide
pPGCs	Presumptive primordial germ cells
P-TEFb	Positive transcription elongation factor b
SP	Side-population
SPG	Shirasu porous glass
SSCs	Spermatogonial stem cells
TEM	Transmission electron microscopy
WL	White Leghorn
ZGA	Zygotic genome activation

CHAPTER 1

GENERAL INTRODUCTION

Avian models have tremendous value as ex vivo-model systems for both basic and clinical purposes, enabling monitoring of cell differentiation, transformation, and organogenesis under specific conditions. Indeed, very little information on early development before oviposition has been reported in comparison with that available after laying of stage X. Although lots of information on cell-fate determination occurring in early embryogenesis was given in a variety of invertebrate and vertebrate species, detailed observation during intrauterine stages in chicken has not been reported to date. Studying initial developmental stages are very important to trace origin of germ cells and to find cell-fate determination in chicken.

Germ cell specification has been explained by two major mechanisms; preformation and induction. In the preformation mode, maternally inherited germplasm has a crucial role for germ cell specification in initial developmental stages, while in the induction mode, germ cells are induced by signals from neighboring somatic cells during gastrulation, as studied in mouse. Chicken primordial germ cells were initially thought to originate from the epiblast. After that, germplasm structure with CVH protein was identified during oogenesis and intrauterine stages. Based on above studies in the history, it seems that chicken germ cells may be specified by maternally inherited determinant (preformation). However, to understand mechanisms of germ cell specification in chicken, additional studies will be needed by using other reliable germ cell-specific markers and transplantation studies during intrauterine stages.

The continuous maintenance of future generation in living organisms is preserved by germ cell development. Thus, germ cell research is important to advance infertility treatments and perform developmental studies.

Elimination of endogenous germ cells has been widely used in germ cell transplantation studies (for clinical purposes) and germline chimera production (for research purposes). Until recently, busulfan treatment was the preferred method of eliminating germ cells. Primordial germ cells (PGCs) are the precursors of germ cells in most vertebrates and play an important role in early embryonic germ cells. Elimination of PGCs by busulfan administration can be performed in early chicken embryos because isolation and manipulation of PGCs from these embryos is simple compared to other vertebrate embryos. However, little about the cellular responses of PGCs after busulfan treatment is known.

To understand the mechanism and potential of avian PGCs, a series of experiments were conducted. In CHAPTER 2, we review the developmental characteristics of chick embryos during intrauterine stages, the biological mechanisms for germ cell specification in birds and other species. Furthermore, the potency of PGCs during their development will also be discussed. In CHAPTER 3, we report differences in sperm dynamics and cleavage events in chick embryos. In CHAPTER 4, we demonstrate the specification of chicken PGCs and germplasm dynamics. Finally in CHAPTER 5, the potency for restorable proliferation of chicken PGCs is discussed.

CHAPTER 2

LITERATURE REVIEW

1. Early Embryo Development in chicken

1.1. Importance of studying intrauterine-embryo development in chicken

Avian species have great value as ex vivo-model for both basic and applied science, enabling monitoring of cellular differentiation, transformation and organogenesis under *in vitro* culture condition. Although chicken has been studied in developmental biology during long time, little information before oviposition exist so far compared to later stages (Stern, 2005). Several problems make it hard to study intrauterine chicken embryos, such as small germinal disc compared to a large amount of yolk and difficulty in intrauterine egg retrieval. Considering the evolutionary important position of chicken for the comparative studies among species, studying intrauterine-embryo development in chicken is obviously important for developmental biology.

1.2. Fertilization and initiation of development in chicken

In chicken, fertilization occurs in the infundibulum after ovulation. And an embryo starts to develop three hours later as the male and female pronuclei fuse (Perry, 1987). Once the oocyte is ovulated, it moves along the oviduct tract for 23-24 hours before it is expelled from the body, which is termed oviposition. The entrance of the oviduct is called infundibulum and the opening is shaped like a funnel which actively engulfs the mature, ovulated ovum. The egg spends up to 20 minutes in the infundibulum and moves into the second part of the oviduct, called magnum following fertilization. In here, the egg-white proteins, called egg albumens are secreted and deposited on the

egg as it travels down this region for about 3 hours. The following part is called isthmus, the site of outer and inner shell membrane formation and the egg spends about 1.5 hours. And ovum spends approximately 18-19 hours in shell gland where most of intrauterine embryo development occurs.

The first division occurs in the isthmus five hours after fertilization (Olsen, 1942). Eyal-Giladi and Kochav analyzed pre-streak embryos and made the staging system based on their duration in uterus and morphological features (Eyal-Giladi and Kochav, 1976). They divided the early embryos into fourteen stages. Among the stages, EGK I to EGK X includes the intrautierine stages. EGK I to VI are collectively called cleavage stages, and EGK VII to X are collectively called formation of area pellucida. The discoidal and meroblastic cleavage continues very rapidly for 12-14 hours, exhibiting a very irregular cleavage pattern. The subgerminal cavity arises at EGK III and cell layers start to increase to reach 5-6 cells thickest at EGK V-VI. During the next 5-7 hours, cells are shed from the ventral side of embryos, the process that starts from the posterior to anterior side. At EGK X, finally, the number of cell layers becomes 1-2 in the area pellucida, while the area opaca remain multilayered. At this stage of development (EGK X; so called oviposition), the egg is laid.

One of interesting characteristics in the avian early development is polyspermy. Polyspermy or supernumerary sperm are not a common phenomenon in mammals, causing the embryonic death with an abnormal ploidy (Snook et al., 2011). However, they are consistently observed in birds (Snook et al., 2011). Chick embryos can develop normally even after the penetration of numerous sperms, suggesting that polyspermy maybe play a role during initial development in chick (Birkhead et al., 1994). The number

of supernumerary sperm nuclei was also investigated showing about average 10-30 nuclei (Patterson, 1910; Fofanova, 1965). Considering the relatively small germinal disc area compared to the entire egg, polyspermy is thought be necessary to ensure successful fertilization (Snook et al., 2011). Also, previous reports showed that low sperm penetration reduces the fertilization rate in chicken (Bramwell et al., 1995; Wishart, 1997). However, detailed information about their dynamics and functions are unknown.

1.3. Maternal determinants and zygotic genome activation (ZGA)

Cell fate determination in an early embryo is governed by two different mechanisms among species. A cell can be specified autonomously by maternal determinants or conditionally by induction signals from surrounding cells. The maternal genome regulates most of early embryonic development in various animal species. Maternal mRNAs and proteins, which are stored in the mature oocyte during oogenesis, regulate the first division and determine initial cell fate and embryonic patterning. During the maternal-to-zygotic transition (MZT), two closed related processes occur successively. First, the maternal mRNAs are gradually eliminated, and second, the transcription of zygotic mRNAs starts (Tadros and Lipshitz, 2009). These two processed are closely related, because zygotic proteins and miRNAs are also involved in degradation of maternal mRNAs.

There were several works about maternal determinant for cell specification in chicken. For example, chicken *vasa* homolog (CVH) protein is co-localized with mitochondrial cloud in the growing oocyte, localized in cleavage furrows and finally several cells of a cleavage embryo that indicates

chicken may use maternally inherited determinant for germ cell specification (Tsunekawa et al., 2000). Also, Callebaut reported early embryo patterning in quail and chicken may be determined by asymmetric distribution of different ooplasms (Callebaut, 2005). However, whether maternal determinants contribute to the lineage segregation and the embryo patterning is still debated.

Zygotic genome activation (ZGA) means the onset of zygotic transcription, the second event of MZT. The timing of ZGA onset is known to be regulated by four different mechanisms including nucleocytoplasmic ratio, maternal clock, abortion of transcript and chromatin regulation (Tadros and Lipshitz, 2009). Also, ZGA occurs in successive waves including minor and major waves. In the mouse, for example, minor ZGA starts at one cell stage and major one starts at 2-cell stage (Wang and Dey, 2006). Information about ZGA gives many clues to understand following embryo development.

To find out the role of ZGA, several experiments were conducted to inhibit the general transcription by drugs or genetic manipulation. For example, after alpha-amanitin treatment, which is an inhibitor of RNA polymerase II, mouse embryos stop the cleavage progression at two-cell stage (Braude et al., 1979). In drosophila, similar treatment causes the inhibition of cellularization at the time of major ZGA groove (Edgar and Datar, 1996). In both frogs and zebrafish, zygotic transction is important for gastrulation after the mid-blastrular transition (MBT) (Newport and Kirschner, 1982; Zamir et al., 1997).

In chicken, however, no study is done about ZGA, so far. One putative ZGA time-point can be EGK VI-VII as formation of area pellucida

starts at EGK VII (Eyal-Giladi and Kochav, 1976). It is quite reliable because the onset of ZGA is related to mid-blastula transition (MBT), that is the end of cleavage stage and onset of major ZGA groove (Tadros and Lipshitz, 2009).

1.4. Hypoblast formation and cell layer dynamics

During intrauterine stages, cell layers change dramatically in chicken. Cell layers form from EGK III-IV by vertical division, reach the maximum 5-6 cell thickness at EGK VI-VII and finally become 1-2 cell thickness at EGK X. Cell layer reduction is thought be caused by cell shedding (Kochav et al., 1980; Fabian and Eyal-Giladi, 1981). But there are also other possibilities including massive apoptosis or compaction of cells. Cell layer reduction is also closely related to hypoblast formation. It is reported that the primary hypoblast arise by poly-ingression from epiblast (Weinberger et al., 1984). Considering 5-6 cell layers at EGK VI-VII, however, it is possible that the hypoblast may already exist early than EGK X. To clarify this, expression pattern of lineage-specific genes should be investigated.

1.5. Conclusion

Studying intrauterine embryos in chick has not been studied well recently in molecular level that makes it the treasure house for developmental biology. Also, previous studies were conducted mainly based on a histological view. Now, therefore, it should be studied to find out what biological mechanisms on there by developed techniques in molecular biology. When the lineage segregation starts, how it is regulated, when the genome is activated and whether there is the contribution of materials of yolk are the major

problems. Studying these fields can help us to understand embryo development in the comparative view across various species.

2. Origin of Avian Germ Cells

2.1. Biology of primordial germ cells

In most multicellular species, only germ cells can transfer genetic and epigenetic information to next generations, thereby being called immortal cells in the body. Because of their unique and important functions for maintaining firm integrity, germ cells are differently regulated from somatic cells at early developmental stages.

The first germline cell population is called primordial germ cells (PGCs) in various species (Saitou and Yamaji, 2010). In most animals, germ cells can be specified either by maternally inherited determinants (preformation mode) or by induction from pluripotent embryonic cells (induction mode) (Extavour and Akam, 2003). Regardless of their mode of specification, PGCs migrate actively and colonize the developing gonads (Richardson and Lehmann, 2010). After settling down in gonads, PGCs differentiate and undergo spermatogenesis in male or oogenesis in female.

Based on their own purpose to generate functional gametes by complex differentiation program, PGCs have unique characteristics during their development. During their specification, PGCs show repressed genome to preserve the important developmental potential of the germline (Nakamura and Seydoux, 2008). In C. elegans and Drosophila, pie-1 (pharynx and intestine in excess) and polar granule component (pgc) block mRNA transcription in PGCs during their specification, respectively (Hanyu-Nakamura et al., 2008; Mello et al., 1996). pie-1 and pgc inhibit

transcriptional elongation by inhibiting P-TEFb (positive transcription elongation factor b) (Ghosh and Seydoux, 2008; Hanyu-Nakamura et al., 2008). Although there is the different mode of specification in mice compared to worms and flies, PGC specification in the mouse also needs transcriptional repression (Nakamura and Seydoux, 2008). Blimp1 (B-lymphocyte-induced maturation protein 1, also known as Prdm1) is responsible for the repression of somatic genes during specification in the mouse (Kurimoto et al., 2008).

Also, because PGCs arise set aside from developing gonads, they have to actively migrate across the embryo (Richardson and Lehmann, 2010). There are different migration pathways among various species. In chicken, PGCs enter extraembryonic blood vessels via blood islands formed at HH 10-12, and circulate in the blood stream until settling down to the genital ridge (Ando and Fujimoto, 1983; Hamburger and Hamilton, 1951; Ukeshima et al., 1991). In mammal, however, PGCs migrate through the embryonic tissues to reach to the gonad (Anderson et al., 2000). In particular, mouse PGCs begin to be polarized after E 7.5 and extend cytoplasmic protrusions to penetrate cell monolayers (Anderson et al., 2000).

Besides above studies, there has been different research fields on PGCs based on their unique characteristics. How they proliferate, what kinds of signaling pathways are involved in PGC proliferation and survival is one of major interests. Many studies focused on growth factors controlling PGC survival and proliferation. In in vitro studies, SCF, LIF, IL4 and CTNF were identified to be involved in PGC survival through suppressing apoptosis (Cheng et al., 1994; Cooke et al., 1996; De Felici and Dolci, 1991; Pesce et al., 1993). Also, bFGF, TNFα and BMP4 can promote the proliferation of PGCs (Choi et al., 2010; Kawase et al., 1994; Pesce et al., 2002; Resnick et al.,

1992). In in vivo studies, SCF/KIT interaction and SCF in combination with FGFs were identified to be involved in survival and proliferation in PGCs (Kawase et al., 2004; Runyan et al., 2006).

2.1.1. PGC-specific and -enriched genes and their regulations

During their development, PGCs strongly express several key genes to regulate the germline competency including transcription factors, RNA-binding proteins, cell adhesion molecules and miRNAs (Saitou and Yamaji, 2010).

During specification, transcription factors such as *Blimp1*, *Prdm14, Tcfap2c* and *Pouv* are strongly expressed in PGCs to repress somatic program and for their survival (Kehler et al., 2004; Yamaji et al., 2008; Ohinata et al., 2009; Weber et al., 2010). When these genes are disturbed, PGCs undergo apoptosis or show impaired specification. Also, *Cdh1*, known as a hemophilic cell-cell adhesion molecule, is involved in PGC specification (Okamura et al., 2003).

There are also important genes regulating proliferation and survival in PGCs. *Scf*, known as a short-chain helical cytokine, is known to role for proliferation, survival and migration in PGCs (Mccoshen and Mccallion, 1975). Receptor molecules such as kit (a receptor tyrosine kinase) and *Cxcr4* (a G-protein-coupled receptor) are also important for proliferation, survival and migration in PGCs (Mintz and Russell, 1957; Ara et al., 2003).

One of important characteristics in PGCs is the expression of

pluripotency-related genes. These genes are first expressed in early pluripotent embryonic cells, and the expression is restricted to PGCs after their specification. PGCs express several pluripotency-related genes including *Pouv*, and *Nanog* during their development and the mis-regulation of these genes cause apoptosis in PGCs (Kehler et al., 2004; Chambers et al., 2007; Okamura et al., 2008).

Also, RNA-binding proteins (RBPs) have been known to have an important conserved role in primordial germ cells among various species. Elimination of *Nanos* and *Dnd1* cause the reduced number of PGCs at E 8.0 and loss of PGCs in the mouse (Sakurai et al., 1995; Tsuda et al., 2003; Suzuki et al., 2008; Cook et al., 2009). Also, *Mvh* (*mouse vasa homolog*)-knockout mice showed impaired PGC proliferation in male after E 11.5 (Tanaka et al., 2000). Besides, Dicer-deleted mice showed impaired PGC proliferation indicating the importance of miRNA-regulation on PGC proliferation (Hayashi et al., 2008). Despite different time of action of the RBPs, it is evident that they play an important role across germ cell development.

Recently, many studies in genomic research areas are focusing on small non-coding RNAs including miRNA, siRNA, shRNA and piRNA and their functions. In particular, there are several woks on miRNA functions on PGCs (Hayashi et al., 2008). miR-290-295 clusters have an important role for PGC migration and survival, and miR-181a maintain undifferentiated properties of PGCs by posttranscriptional regulation (Lee et al., 2011; Medeiros et al., 2011).

2.1.2. PGC specification in general

Understanding the mechanisms of germ cell specification is the major challenge in the fields of evolutionary and developmental biology, because only germ cells can transfer genetic and epigenetic information across whole generations in most animal species. In particular, how and when germ cells are segregated from the somatic lineage are crucial problems.

Because of complicated dynamics of germ cell development, it is needed to mention nomenclature on germ cells. In this review, we will follows the terminology of Nieuwkoop and Sutasurya (Nieuwkoop and Sutasurya, 1979), followed by Extavour and Akam (Extavour and Akam, 2003). Sexually differentiated germ cells of first stages of gametogenesis are termed gonia. During the gametogenesis, gonia become oocytes and spermatocytes and finally become ova and spermatozoa. Primordial germ cells (PGCs) indicate the first cells that will give rise to gonia (or germline stem cells) by clonal mitotic divisions. Also, the precursors of the PGCs which are often morphologically indistinguishable from the neighboring somatic cells are called presumptive primordial germ cells (pPGCs) (Extavour and Akam, 2003).

Germ cell specification has been known by two major mechanisms; preformation and induction mode. In the preformation mode, maternally inherited germplasm containing mRNAs, proteins and small RNAs play a crucial role for germ cell specification in initial developmental stages. On the other hand, in the induction mode, germ cells are induced by signals from neighboring somatic cells during gastrulation. Despite distinct mechanisms of

action, several characteristics of PGCs are conserved regardless of the modes of specification. First, PGCs have large round-shape nucleus and cytoplasmic granules. Second, electron-dense structures in the cytoplasm of germ cells are observed in most of species revealed by transmission electron microscopy (TEM). Third, PGCs express several specific molecular markers including enzymes, adhesion molecules and RNA-binding proteins that are conserved among species. Also, germ cells often exhibit the transcriptionally inactive status to maintain germ cell integrity during early development.

"Germ granules" indicates cytoplasmic bodies of germ cells containing mRNAs, proteins, small RNAs and others. One of important characteristics of germ granules is electron-dense structures under TEM without membrane. The mRNAs, proteins and small RNAs in germ granules play a role for specification, germ-cell specific expression and post-transcriptional regulation in germ cells. In some organisms like *C. elegans* and *Drosophila*, germ granules are maternally inherited from oocyte to embryo for germ cell specification. While in other organisms like mouse, they are present in later germ cell after specification rather in oocytes and early embryo. So far, it is concluded that germ granules are present in all organisms and play an important role for germ cell development regardless of mode of specification.

2.1.2.1. Preformation mode

In *Drosophila melanogaster*, posterior pole cells will give rise to germline cells (Technau and Camposortega, 1986; Williamson and Lehmann, 1996). Before fertilization, pole plasm is assembled in the posterior region of

the oocyte, and the pole cells will have the pore plasm after celluarization (Mahowald, 2001). To identify the function of the pole plasm, transplantation or forced assembly of the pole plasm was conducted (Illmense.K and Mahowald, 1974; Illmensee and Mahowald, 1976; Ephrussi and Lehmann, 1992). Remarkably, transplantation of pole plasm into non-posterior region caused ectopic PGC formation, which indicates that the pole plasm is a real functional germ cell determinant.

In *Caenorhabditis elegans*, electron dense granules called P granules are scattered throughout the cytoplasm before fertilization, but then move to the posterior part of the embryo during zygote formation (Hird et al., 1996). During early embryo development, the P granules are distributed asymmetrically so that the P_4 blastomere of 16-24 cell stage harbors all of them, and become the PGC (Deppe et al., 1978; Strome and Wood, 1982). Even in other nematodes, the P_4 cell always becomes the PGC, indicating maternal inheritance of the germplasm is conserved in nematodes.

Besides insects, there are several vertebrate species that select the preformation mode of specification. One example is *Xenopus laevis*. As in flies and worms, germplasm is assembled during oogenesis and localized to the vegetal subcortex of *Xenopus laevis* (Bounoure, 1939). In the germplasm, mitochondria, proteins and RNAs are accumulated (Heasman et al., 1984; Houston and King, 2000; Kloc et al., 2001). During cleavage stages, the vegetal plasm forms patch-like structures and asymmetrically segregated, and finally accumulate in some cells that will become the PGCs (Whitington and Dixon, 1975). The vegetal plasm also has germ cell determinants that was confirmed by removal or transplantation studies (Nieuwkoop and Suminski, 1959; Smith, 1966; Ikenishi et al., 1974).

Another example is Danio Rerio. *Vasa* mRNA, which is one of germplasm components, is synthesized during oogenesis and localized to the cleavage planes of the 1st cleavage stage embryo. Then, *vasa* mRNA is restricted to only four cells in the 32-cell stage embryo, the four cells become the PGCs (Yoon et al., 1997).

2.1.2.2. Induction mode

The induction mode of specification is conserved in most mammalian species. Although there were debates during early studies about germ cell specification in mammals (Heys, 1931; Everett, 1945), it is proved that the germ cells in mammals are specified by inductive signals. Despite the germline specific expression and important function of *mvh* (mouse *vasa* homologue), it is not localized to a specific region in oocytes during oogenesis, indicating on germ plasm is formed (Fujiwara et al., 1994; Toyooka et al., 2000; Noce et al., 2001). Cells from the distal epiblast can differentiate into PGCs when transplated into the proximal epiblast where the PGCs arise in mammals. However, the proximal epiblast cells can not differentiate into PGCs when transplanted to the distal epiblast, that indicates that there is the inductive signals for germ cell specification in the mouse (Tam and Zhou, 1996). One of major signal molecules for germ cell specification is the bone morphogenetic proteins (BMPs). The expression of *Bmp4*, *Bmp8b* and *Bmp2* is known to be required for germ cell induction in the mouse (Lawson et al., 1999; Ying et al., 2000; Ying and Zhao, 2001). Also, several cells in the proximal epiblast express *fragilis* and *stella*, which can make the cells to respond BMP signals (Surani et al., 2002).

2.2. PGC specification in chicken

Since early 1900th, origin of germ cells in birds is one of major problem in germ cell biology. Despite lack of reliable markers for PGCs in the early studies, lots of reliable information has accumulated by the pioneers. And chicken has been used for the representative model among avian species in many studies.

Chicken primordial germ cells were first identified in the germinal crescent region and thought to originate from the hypoblast (Swift, 1914). In this study, PGCs were identified by morphological characteristics such as a large amount of glycogen granules in the cytoplasm and a large cell size compared to the surrounding somatic cells. Because of a large content of glycogen granules, the following studies used the periodic acid Schiff (PAS) staining to distinguish the PGCs (Meyer, 1964; Ginsburg et al., 1989).

At late nineteenth, however, Eyal-Giladi and others showed the epiblastic origin of PGCs by the chick-quail chimera study (Eyal-Giladi et al., 1981). Based on this study, the following works were focused on the induction mode of specification at around EGK stage X (Karagenc et al., 1996; Naito et al., 2001). Also, it is evident that only the central region of the blastoderm at stage X can give rise to PGCs (Ginsburg and Eyal-Giladi, 1987; Naito et al., 2001). It was quite reliable that chicken PGCs arise at around EGK stage X by inductive signals, because there had been no evidence of the germplasm existence during cleavage stages even in quail (Ginsburg et al., 1989).

However, at 2000, a chicken *vasa* homologue (*CVH*) was isolated,

and chicken PGCs were traced backwards to initial developmental stages (Tsunekawa et al., 2000). Remarkably, CVH protein is co-localized with spectrin and mitochondrial clouds in the growing oocytes that indicates the presence of germplasm in chicken. Also, CVH protein is localized to cleavage furrows and restricted to only six to eight cells of 300-cell stage embryo as a patch-like structure.

Above data suggest that chicken germ cells may be specified by maternally inherited determinant (preformation). However, additional studies will be needed to clarify the mode of germ cell specification in chicken using other reliable germ cell-specific markers and transplantation studies during intrauterine stages.

3. Potency of germ cells

3.1. Introduction of germ-cell potency

Germ cells initiate to develop from early developmental stages and give rise to functional gametes such as sperm and ovum. During their development and differentiation, germ cells show dynamic changes of morphology, gene expression and molecular behaviors. Germ cells are also called differently based on their developmental status including presumptive primordial germ cells (pPGCs), PGCs, germline stem cells (GSCs), spermatogonia and oogonia, spermatocyte and oocyte, and sperm and ova. Among them, several populations are identified to have the potential that is the capability of self-renewal and differentiation under specific conditions.

3.2. Potency of primordial germ cells

PGCs, the precursor of functional gametes, are known well to have the potency that can give rise to pluripotent stem cells under specific circumstances. In mouse and human, when PGCs are cultured with a specific cocktail of growth factors including KL, LIF and FGF2, they dedifferentiate into pluripotent stem cells, called embryonic germ cells (EGCs) (Matsui et al., 1992; Resnick et al., 1992; Shamblott et al., 1998). The mouse EG cells can differentiate into three germ-layer cells after transplantation.

It is also reported that there is a side-population (SP) of PGCs in mice (Scaldaferri et al., 2011), which have a greater ability to develop into pluripotent stem cells that indicates subpopulation of PGCs (Matsui and

Tokitake, 2009). In addition, SP cells that differentiated from PGCs were enriched in spermatogonia of developing mice testes (Lassalle et al., 2004).. Consistent with above results, conserved expression of several pluripotency-related genes and microRNAs were identified in PGCs (Yeom et al., 1996; Kerr et al., 2008; Lee et al., 2011).

Chicken PGCs can also give rise to EGCs under the specific conditions, and make functional gametes to produce donor-derived progeny from germline chimeras (Park and Han, 2000; Park et al., 2003). Besides, chicken PGCs can be cultured *in vitro* for a long time and produce donor-derived progeny from germline chimeras (Choi et al., 2010; Macdonald et al., 2010). However, the SP population in chicken has not been reported yet.

3.3. Potency of germline stem cells

Germline stem cells in testis, which is also called spermatogonial stem cells (SSCs), are derived from PGCs, and have a capability of self-renewal by clonal expansion. The initial population of GSCs provides whole germline cells in the testis. Pluripotency of germline stem cells (GSCs) is well demonstrated in the mouse (Brinster and Zimmermann, 1994; Kanatsu-Shinohara et al., 2004; Guan et al., 2006). In the testis, only about 0.03% of germ cells has a reconstitution potential after transplantation and are demonstrated as GSCs. Also, GSCs can be reprogrammed and dedifferentiated into embryonic stem cell (ESC)-like cells and give rise to all three germ layers *in vitro* (Guan et al., 2006; Guan et al., 2007).

3.4. Effects of chemotoxic agents on germ cells and its use

Based on the potency of germ cells, elimination of endogenous germ cells has been widely used in germ cell transplantation studies for regenerative medicine and germline chimera production. Several experimental methods including γ-ray irradiation, x-ray irradiation (Campion et al., 2010; Park et al., 2010) and busulfan administration (Song et al., 2005; Lee et al., 2006; Nakamura et al., 2010) to eliminate endogenous germ cells in different vertebrate species have been developed. These methods primarily induce DNA damage in target cells, resulting in loss of all cellular mechanisms and ultimately cell destruction.

Busulfan, an alkylating agent, has been used for clinical studies of chronic myelogenous leukemia and bone marrow transplantation (Down and Ploemacher, 1993; Buggia et al., 1994). Generally, busulfan is known to targets slowly proliferating and non-proliferating cells. The mechanism of action of busulfan has been identified as DNA alkylation leading to DNA–DNA cross-linking (Iwamoto et al., 2004), which causes cell death and/or cellular senescence through the ERK and p38 pathways. Busulfan also functions as a mitogen-activated protein kinase (Probin et al., 2007).

Until recently, busulfan treatment was the preferred method of eliminating germ cells. Although busulfan administration can induce side effects including lethality, sterility and teratogenicity (Bishop and Wassom, 1986), the majority of studies have applied busulfan to eliminate germ cells in mouse and rat testis because of its relatively higher cytotoxicity to target cells. After busulfan administration, testicular germ cells undergo apoptosis; however, small population of spermatogonial stem cells (SSCs) survive in mice (Choi et al., 2004). These surviving SSCs may be involved in restoration of the germ cell population after reduction or withdrawal of busulfan toxicity

(Zohni et al., 2012).

Primordial germ cells (PGCs) are the precursors of germ cells in most vertebrates and play an important role in germline chimera studies (Han, 2009). Elimination of PGCs by busulfan administration can be performed in early chicken embryos because isolation and manipulation of PGCs from these embryos is simple compared to other vertebrate embryos. In chickens, PGCs originate in the epiblast and migrate through the hypoblast and blood to reach embryonic gonads. Busulfan administrated into chicken eggs at Eyal-Giladi and Kochav (EG&K) stage X successfully eliminated all endogenous PGCs in the embryos. After busulfan treatment, donor PGCs injected into the embryos migrated and colonized on the recipient gonads. The proportion of donor-derived offspring was also increased significantly (Nakamura et al., 2008). However, little about the cellular responses of PGCs after busulfan treatment is known.

CHAPTER 3

Cleavage Events and Sperm Dynamics in Chick Intrauterine Embryos

1. Introduction

Avian models have tremendous value as ex vivo-model systems for both basic and clinical purposes, enabling monitoring of cell differentiation, transformation, and organogenesis under specific conditions. Nevertheless, limited work has been conducted due to technical difficulties in egg retrieval before oviposition. Furthermore, avian embryos demonstrate discoidal meroblastic cleavage with a large amount of yolk and a small germinal disc (Patterson, 1910; Olsen, 1942), which hinders monitoring early embryo development. Indeed, very little information on early development before oviposition has been reported (Bellairs et al., 1978; Bakst et al., 1997; Park et al., 2006) in comparison with that available after laying of stage X (Eyal-Giladi and Kochav, 1976). In this study, we employed a non-surgical intrauterine egg collection by abdominal rubbing (Eyal-Giladi and Kochav, 1976), which contributes to overcoming current technical limitation.

Lots of information on cell-fate determination occurring in early embryogenesis was given in a variety of invertebrate and vertebrate species (Plusa et al., 2005; Zernicka-Goetz et al., 2005; Zernicka-Goetz, 2005). Differing from mammals, polyspermic penetration was physiologically occurred in avian eggs, but detailed observation has not been reported to date. In this study, we employed a non-invasive egg retrieval technique with comparative classifying of egg shall formation and embryogenesis for monitoring details of sperm penetration and early cleavage events.

2. Materials and methods

Experimental animals

White Leghorn (WL) hens (54–56 weeks old) were used for the collection of intrauterine eggs. We managed chickens according to our standard operation protocol. Relevant experimental procedures for the study were approved by the Institutional Animal Care and Use Committee, Seoul National University before undertaking experiments (SNU-070823-5).

Collection of intrauterine eggs from hens

Intrauterine eggs retrieved from WL hens were harvested by an abdominal massage technique slightly modified from Eyal-Giladi and Kochav (Eyal-Giladi and Kochav, 1976). Briefly, the abdomen of hens was pushed gently until exposure of the shell gland, and the surface of the shell gland expanded when an egg was located there for eggshell formation. After expansion of the surface of the shell gland, massage was used to move the egg gently toward the cloaca until the intrauterine egg was released (Fig. 1A).

Analysis of cleavage stages in the intrauterine embryos

Intrauterine embryos were separated from the egg using sterilized paper (Chapman et al., 2001) and the shell membrane and albumen were detached from the yolk. A piece of square-type filter paper (Whatman, Maidstone, Kent, UK) with the hole at the center was placed over the germinal disc. After cutting around the paper containing the intrauterine

embryo, it was gently turned over and transferred to saline buffer to further remove the yolk and the vitelline membrane for embryo collection (Pannett and Compton, 1924). Collected embryos were fixed with 4% (w/v) paraformaldehyde in 1× phosphate-buffered saline (PBS) and the fixed embryos were classified according to the cleavage stages proposed by Eyal-Giladi and Kochav (Eyal-Giladi and Kochav, 1976). Unfertilized and abnormal embryos were identified by the morphological criteria of cleavage furrows.

Photographs of the dorsal part of intrauterine embryos were taken with a stereoscopic zoom microscope (SMZ1000; Nikon Corporation, Tokyo, Japan) and EG&K stage I-II embryo was cultured in Chamlide incubator system (Live Cell Instrument, Seoul, Korea) at 41.5 °C with 5% of CO_2 gas for live cell imaging. Shell membrane- and albumen-detached eggs were put into the 25 ml plastic cup (40025; SPL Life Sciences, Pocheon, Korea) with 10 ml of albumen on the bottom and the surface area on the top was covered with 3 ml of albumen. For retaining embryo viability, all procedures were undertaken less than five minutes in the heated room (more than 30 °C). Time-lapse images were taken by multi-purpose zoom confocal microscope (AZ100; Nikon Corporation, Tokyo, Japan).

Phalloidin and DAPI staining of intrauterine embryos

After fixation with 4% paraformaldehyde, the intrauterine embryos were washed in PBS three times and incubated in 0.1% (v/v) Triton X-100 in PBS (PBST). The fixed embryos were incubated with Alexa Fluor 488 phalloidin (A12379; Invitrogen, Carlsbad, CA, USA) diluted 1:40 in PBST overnight at room temperature. After overnight incubation, the embryos were

washed three times in PBS and mounted with Prolong Gold antifade reagent with 4',6-diamidino-2-phenylindole (DAPI) (P36931; Invitrogen). The stained embryos were observed under a fluorescence microscope (Ti-U; Nikon Corporation). In addition, the intrauterine embryos were embedded with paraffin and sectioned (12 μm) using a microtome and after being mounted with Prolong Gold antifade reagent with DAPI, the embryonic nuclei were evaluated under a fluorescence microscope.

Statistical analysis

Statistical analyses were performed using the Student t test in SAS version 9.3 software (SAS Institute, Cary, NC). The significance levels between control and treatment groups were analyzed using the general linear model (PROC-GLM) in SAS software. Differences between treatments were deemed to be significant when P was less than 0.05.

3. Results

Retrieval of intrauterine eggs

The general procedure for the noninvasive collection of intrauterine eggs by abdominal massage is shown in Figure 1. This procedure resulted in minimal stress to the hens, which continued to lay eggs from the second day after harvest. Ninety-five WL hens at 54-56-week-old were provided for egg retrieval, and intrauterine eggs were retrieved from all hens. Among the 95 collected embryos, 38 were of EG&K stage I, 26 of stage II, 11 of stage III, 13 of stage IV, and 7 of stage V. In total, 67.4% of the harvested intrauterine embryos were classified as early EG&K stages I-II. Intrauterine eggs can be divided into three categories based on morphological characteristics (Fig. 1B): eggs with a yellowish soft eggshell membrane of EG&K stages I-V, eggs with a light yellowish flexible eggshell of EG&K stages V-VII, and eggs with a milky-white stiffened eggshell of EG&K stages VII–X. Eggshell formation advanced gradually in the shell gland. The calcium-deposited eggshell was well formed during EG&K stages V-VI (8 h in the shell gland), hardening of the eggshell was observed at EG&K stage VII, and eggshell formation was complete by EG&K stages IX-X. Overall times to retrieve each stage were expected to be 0-8, 8-12, and 12-20 h after entering into shell gland for phases I, II and III, respectively.

Morphogenesis of cleavage furrows in intrauterine embryos

Of the 38 EG&K stage I embryos collected from the shell glands, five were undergoing the first cleavage (Fig. 2A). The first cleavage furrow was observed in the central region, while a few showed the initiation of

cleavage in the peripheral area. Six of the 38 underwent synchronous cleavage up to the third cleavage, perpendicular to the previous cleavage furrow. The fourth cleavage separates central and peripheral cells (schematic diagram; Fig. 2B). Distinguishable from the main cleavage furrows formed in a cruciform manner, peripheral cleavage furrows were formed at the embryo boundary until EG&K stage V (Fig. 2A, C). The peripheral furrows disappeared gradually after EG&K stage V and became invisible. During cell divisions between EG&K stages I and V, cell size decreased gradually and was approximately tenfold smaller (from 250-300 to 15-40 μm) at EG&K stage V than that of the first cleavage stage (Table 1). As shown in Table 1, preblastodermal cells, indicating completely closed cells detached from the yolk, were detected from EG&K stage III, but the size varied due to rapid cleavage after EG&K stage II. The subgerminal cavity was initially formed with completely closed cells beginning at EG&K stage III. At EG&K stage IV, the central cells began to form cell layers, and three to six cell layers were detected at EG&K stage V; at this stage, preblastodermal cells were observed in both the central and the peripheral regions (Figs. 2C, 3A).

To further examine cell division, time-lapse live-imaging of the cleaving embryo (EG&K stage I-II) was taken (Fig. 4). Cleavage of two laterally closed cells at the central region, which were indicated as ‘1’ and ‘2’ in the first panel of Fig. 4A, was monitored during 4 hours of culture. Asymmetric division with asynchronous cleavage was notable in the observation of two cells. The cell surface area of the cell number ‘1’ was 11258.92 μm^2 at onset of culture and those of its daughter cells were 6855.68 and 3711.55 μm^2 at 58 minutes after culture, that indicated asymmetric division in each of the two cells (Fig. 4B left). In terms of cleavage duration, the second division in one of daughter cells of the cell number ‘1’ completed at 144 minutes after the onset of culture, while that in the other daughter cell

completed at 204 minutes after the onset of culture, that indicated asynchronous division (Fig. 4B left). The cell number '2' also showed asymmetric division during culture (Fig. 4B right).

To trace the division direction of open cells, time-lapse live-imaging of the total three cleaving embryos (EG&K stage I) was taken and the one representative embryo is shown in Fig. 5. The embryo had total eight cells including one closed cell and seven open cells and the daughter cells were traced during one cleavage cycle. Two kinds of division of open cells were observed. The cells labeled O1, 3 and 5 made two open daughter cells. However, the cells labeled O2, 4, 6 and 7 divided asymmetrically and made one closed cell and the other open cell. The asymmetric division of open cells was observed in all three embryos. The abnormal embryo development and cell apoptosis were not observed during at least 4 hours of ex ovo culture.

Localization of F-actin to the cleavage furrows and division patterns in intrauterine embryos

Nuclear and F actin staining respectively with DAPI and phalloidin was conducted to examine the cleavage pattern of intrauterine embryos. Strong F actin staining was detected in the main cleavage furrow and in the peripheral area of EG&K stage I embryos (Fig. 6). Subsequently, F-actin was detected strongly in the second and third cleavage furrows. The newly developed cleavage furrows appeared not to be initiated from the dorsal surface, but rather from deeper cytoplasmic regions underneath the surface (Fig. 6A, B). During this early stage, F-actin-stained cleavage furrows from the center did not reach the peripheral area of the embryos (Fig. 6). F-actin-stained peripheral cleavage furrows were formed in an irregular (linear, dot-

shaped, circular) manner (Fig. 6C). From EG&K stage I, the dividing cells in the center became closed first (Fig. 6), whereas the peripheral cells were still open before stage IV. Closed cells in the peripheral area were detected primarily in stage IV, and the majority of cells were completely closed in stage V (Fig. 6H, I). Double-staining with phalloidin and DAPI clearly showed cell division patterns in the intrauterine embryos in EG&K stages II–V (Fig. 6).

Embryonic and supernumerary sperm nuclei in the intrauterine embryos

Three types of nuclei were observed in the intrauterine embryos according to their morphology, size and position: embryonic (zygotic) nuclei, condensed supernumerary sperm nuclei, and decondensed supernumerary sperm nuclei. Condensed sperm nuclei were mainly present in the dorsal surface and cytoplasm, and rarely in the yolk region underneath the cytoplasm (Fig. 3, 7) with a linear shape (Fig. 8B), whereas the decondensed sperm nuclei were spread in the peripheral yolk region and yolk region underneath the cytoplasm (Fig. 3, 7) with an irregular shape and smaller size compared to embryonic nuclei (Fig. 8B). Also, the three-dimensional depth coding image showed that the decondensed sperm nucleus was located under the cytoplasm, while embryonic nuclei were in the cytoplasm (Fig. 8A). Less than ten to several thousand condensed and decondensed supernumerary sperm nuclei were detected in the cleavage stages of intrauterine embryos. In particular, the numbers of condensed supernumerary sperm on the dorsal side of EG&K stages I-III embryos ranged from 1 to 10 to more than 1000 per embryo (Table. 2). However, late EG&K stage embryos contained very low numbers of supernumerary sperm nuclei. It was obvious that observed sperms were penetrated because the vitelline membrane of all embryos was removed before staining. In the yolk on the ventral side, only decondensed sperm heads were

observed in the majority of embryos. In a few embryos, a few condensed sperm heads were also observed on the ventral side as well as decondensed sperm heads.

To examine the spatial distribution of supernumerary sperm nuclei, condensed and decondensed sperm nuclei on the dorsal and ventral side of EG&K stage I-II embryos were counted respectively (Fig. 9). On the dorsal side, condensed sperm nuclei and embryonic nuclei were detectable while decondensed sperm nuclei were present on the ventral side (Fig. 9A2, 9B2). Also, the mean number of condensed sperm nuclei was significantly higher on the periphery region than center region (Fig. 9A3). The number of condensed and decondensed sperm nuclei per 1 mm^2 of cell surface area was shown in Fig. 9A4 and 9B4.

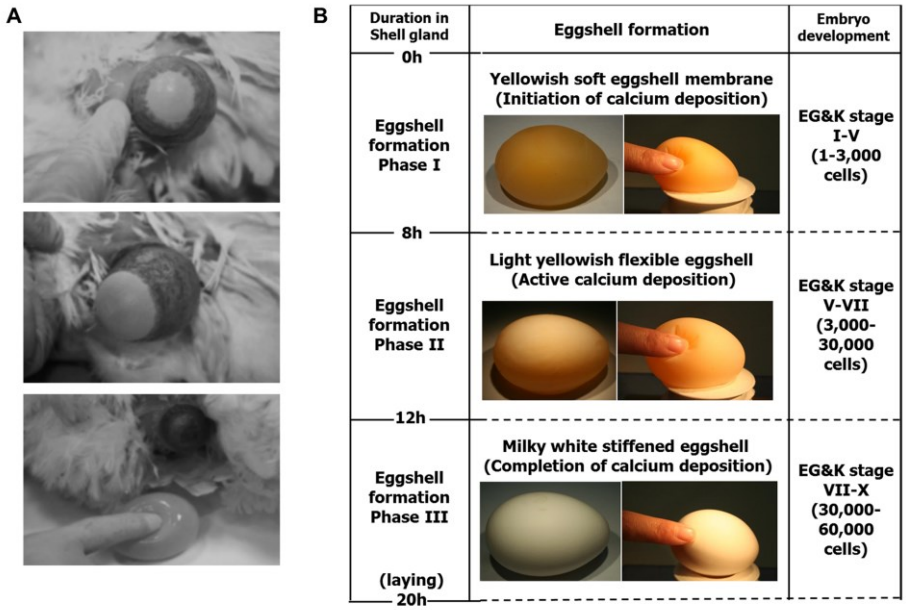

Figure 1. Noninvasive collection and classification of intrauterine eggs by abdominal massage. (A) No surgical manipulation was performed for intrauterine egg retrieval. (B) Phase I, II, and III stages were designated, which were equal to embryonic EG&K stages I–IV, V–VI, and VII–X, respectively. The phase I stage represented as an egg with a yellowish and soft eggshell, phase II was an egg with a light yellow-colored, flexible eggshell, and phase III was an egg with stiffened and calcium-deposited eggshell with a milky-white color.

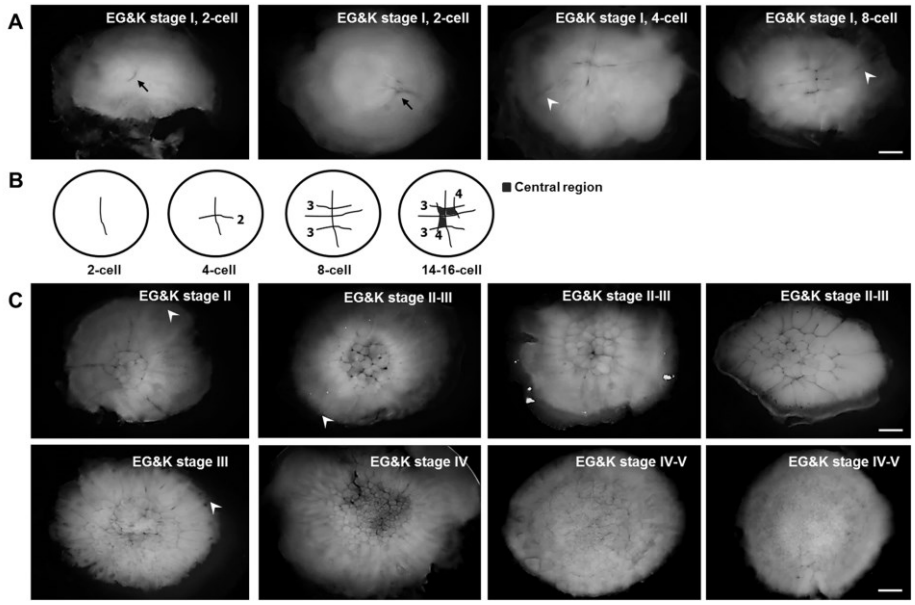

Figure 2. Cleavage of harvested phase I stage eggs in vitro. (A) Formation of cleavage furrows in the EG&K stage I, 2–8-cell embryos. Asymmetric divisions with synchronized cleavage at the early EG&K stage I were observed. (B) Schematic diagram showing the pattern of early cleavage in 2–8-cell embryos. The first two divisions were synchronized and the initial cruciform cleavage yielded four nonpolar preblastodermal cells. (C) Cleavage of EG&K stage II–V embryos. Cleavage proceeded in a radial manner from the cleavage initiation region. Black arrows indicate the first cleavage furrow, and white arrowheads denote cleavage furrows in the peripheral area (scale bar = 500 μm).

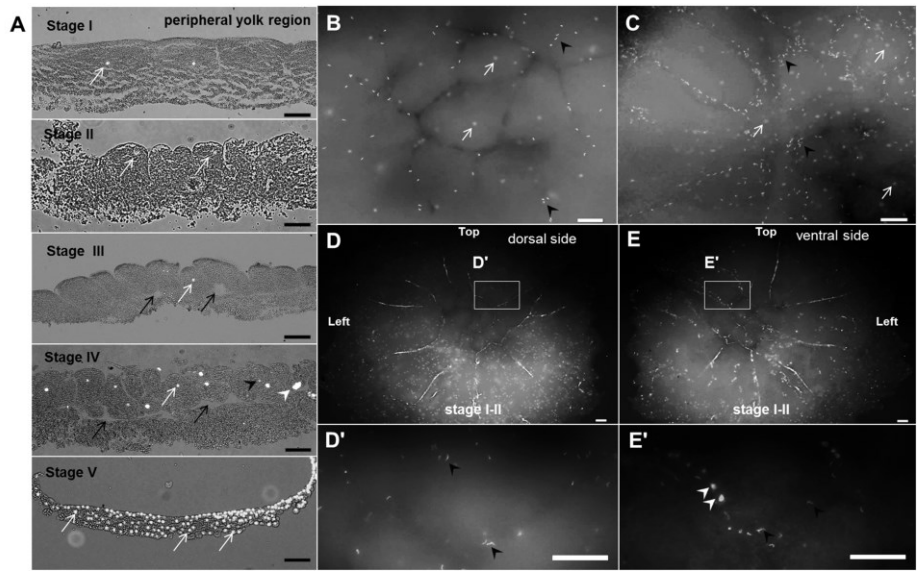

Figure 3. Spatial distribution of condensed and decondensed sperm heads. (A) Relative position of embryonic and sperm nuclei during development (sectioned view). Condensed sperm heads were visible on the dorsal side of EG&K stage I (B) and III (C) embryos. (D) The majority of condensed sperm heads were visible on the dorsal side of EG&K stage II embryos, while decondensed sperm heads were observed on the ventral side (E). In a few embryos, a few condensed sperm heads were also visible on ventral side (E). (D', E') Higher magnification images of (D) and (E). White and black arrows indicate embryonic nuclei and subgerminal cavities, respectively, while white and black arrowheads indicate decondensed and condensed sperm nuclei, respectively. Decondensed sperm heads were present primarily in the yolk and cytoplasmic areas (scale bars = 100 μm).

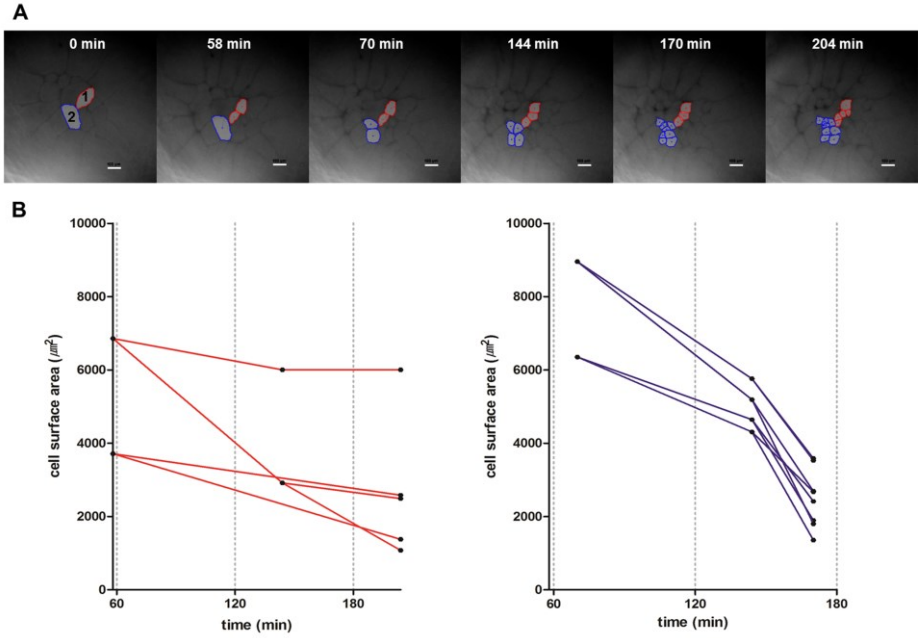

Figure 4. The asynchronous and asymmetric cleavage pattern of the EG&K stage I embryo. The embryo was harvested from the phase I egg stage and cultured in the live-imaging chamber for 4 hours. Time-lapse images were taken by confocal microscope during culture. Cleavage of two adjacent cells at the central region named as '1' (red color) and '2' (blue color) were monitored. (A) Asymmetric division with asynchronous cleavage was notable (scale bar = 100 μm). (B) Changes in cleavage duration and cell surface area in the preblastodermal cells derived from cell number '1' (left) and cell number '2' (right) (X axis = time after culture, Y axis = cell surface area, μm^2). Data demonstrated both the size of preblastodermal cells and cleavage duration were decreased as the cleavage was progressed.

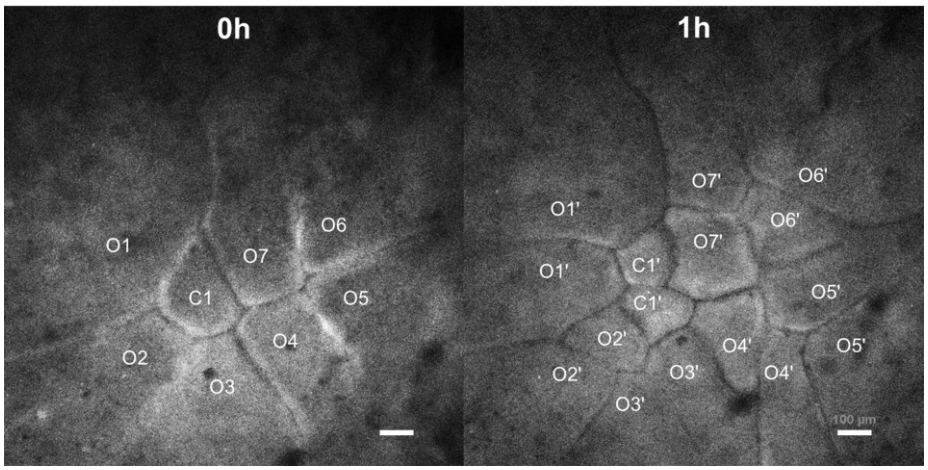

Figure 5. Time-lapse observation on the cleavage of the EG&K stage I embryo in the phase I stage. The embryos were harvested from the phase I egg stage and cultured in the live-imaging chamber. Time-lapse images were taken by confocal microscope during culture. One closed cell (C1) and seven open cells (O1-O7) were present at 0 min and became six closed cells and ten open cells after sixty minutes. The open cells at 0 min divided in two ways; cells labeled O1, 3 and 5 made two open daughter cells, while cells labeled O2, 4, 6 and 7 made one open cell and one closed cell after one cleavage cycle, indicating the division direction of open cells are not fixed (scale bar = 100 μm).

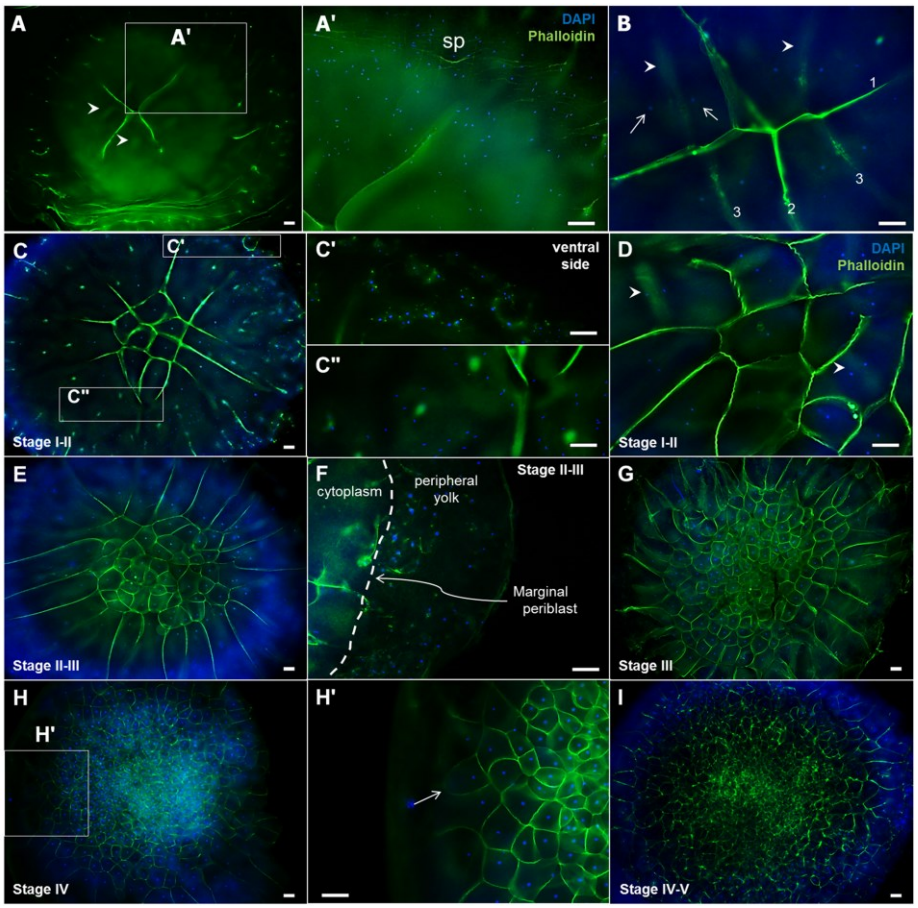

Figure 6. Cleavage pattern in EG&K stage I-V embryos, detected by phalloidin staining. Cleavage of 4-cell embryos was monitored after being harvested (A), and the upper right area (A') was magnified to show many sperm heads appearing as blue spots (Sp: sperm). Cleavage of 8-cell embryos was monitored after being harvested (B). Mitotic nuclei stained with DAPI were observed before cleavage furrow formation (arrows), and the furrow formed after detection of mitotic nuclei (arrowheads). New cleavage furrows developing between two daughter nuclei were observed from the ventral, rather than the dorsal side, showing completion of diakinesis before

cytokinesis. The order of cleavage furrow formation was indicated in Arabic numerals (B). (C, D) Cleavage of EG&K stage I-II embryos were monitored. Multinuclear preblastodermal cells having two daughter nuclei were detected, while due to vigorous proliferation, the size of preblastodermal cells in the cleavage initiation region was smaller than that of the cells in the peripheral region at the initial cleavage stages. Decondensed sperm heads were visible on the ventral side of the embryos (C') and condensed sperm heads were visible on the dorsal side (C") and formation of the large number of cleavage furrows before cytokinesis was visible primarily in the peripheral region (C). Formation of cleavage furrows with mitotic nuclei in stage II was visible (arrowheads in D). (E, F) EG&K stage II–III embryos had many decondensed sperm heads, considered to be penetrated sperm, in the peripheral yolk part. (G, H) Image of EG&K stage III and IV embryos and mononuclear preblastodermal cells were visible. Less formation or closing of cleavage furrows was notable in the peripheral region (arrows) at stage IV (H'). (I) Image of EG&K stage IV–V embryos (scale bars = 100 μm).

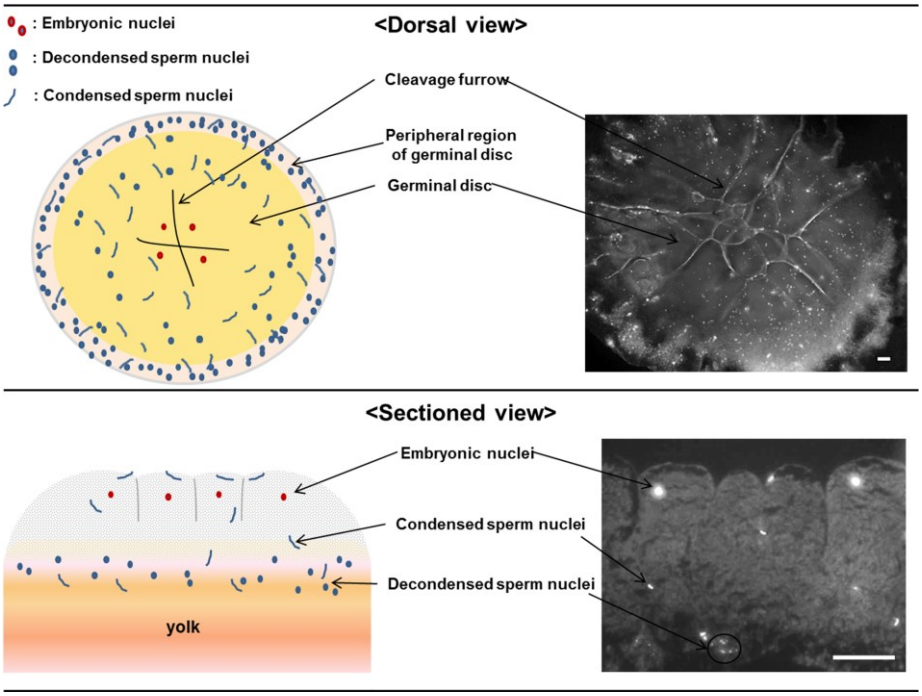

Figure 7. Diagrammatic representation on the position of decondensed and condensed sperm heads. Condensed sperm heads were observed on the dorsal surface in the areas of the germinal disc, cytoplasm, and egg yolk, while decondensed intracytoplasmic sperm heads were observed primarily in the periphery of the egg yolk. Sectioned view (bottom) showed condensed sperm nuclei in the cytoplasm and yolk region. Decondensed sperm nuclei are located in the yolk underneath the cytoplasm (scale bars = 100 μm).

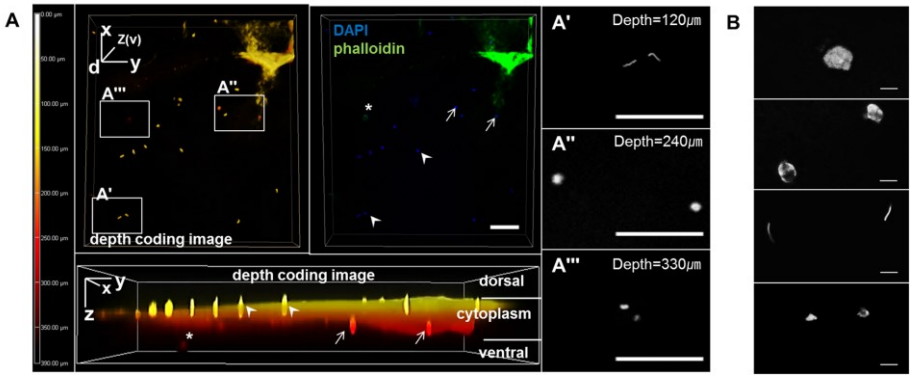

Figure 8. Classification of embryonic nuclei, condensed and decondensed sperm heads by morphology and relative position on the z-axis. (A) Confocal image demonstrated that decondensed sperm heads was present in the yolk under the cytoplasm, while embryonic nuclei were in the cytoplasm. (A'-A''') Higher magnification images of (A) on z-axis of each position. White arrows indicate embryonic nuclei, while arrowheads indicate condensed sperm heads in the surface area. Asterisk denotes decondensed sperm nucleus (scale bars = 100 μm). (B) Morphologies of nuclei present in whole mount embryos stained by DAPI (from top to bottom; embryonic nucleus at interphase, mitotic embryonic nuclei, condensed sperm heads and decondensed sperm heads, scale bars = 10 μm).

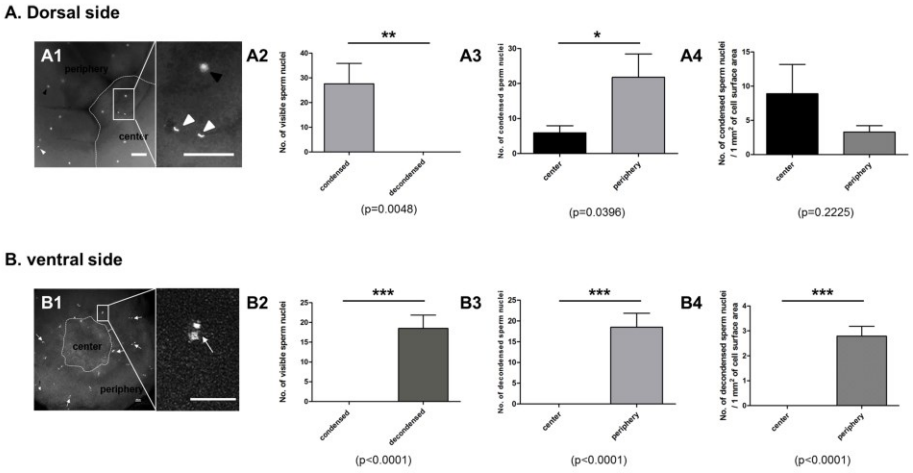

Figure 9. Spatial distribution of supernumerary sperm nuclei on the dorsal side (A) and the ventral side (B) of EG&K stage I-II embryos. (A1 and B1) DAPI stained embryo (scale bars=100μm). On the dorsal side (A1), condensed sperm nuclei and embryonic nuclei were detectable while only decondensed sperm nuclei were detectable on the ventral side (B1). White arrowheads and black arrowheads in A1 indicate condensed sperm nuclei and embryonic nuclei, respectively. Arrows in B1 indicate decondensed sperm nuclei. White dotted line indicates the boundary between the center and the periphery region. The center region and the periphery region were designated for laterally closed cells and open cells, respectively. (A2 and B2) The number of condensed and decondensed sperm nuclei on each side. (A3 and B3) The number of condensed and decondensed sperm nuclei on the center region and the periphery region. (A4 and B4) The number of condensed and decondensed sperm nuclei per 1 mm^2 of cell surface area. Total eight embryos were used for the experiment (n=8).

Table 1. Early morphogenesis of chick embryos before oviposition

	EG&K stage				
	I	**II**	**III**	**IV**	**V**
Duration in shell gland (h)	0–1	2	3–4	5–7	8–9
Preblastodermal cell size (μm)	250–300	90–200	80–150	60–100	15–40
No. of cell layers	1	1	1	2–3	3–6
*Preblastodermal cell formation	Only laterally closed cells in the center	Only laterally closed cells in the center	Preblastodermal cell formation in central region	Preblastodermal cell formation in central region	Preblastodermal cell formation in both central and peripheral regions
Subgerminal cavity	Non-developed	Non-developed	Initially seen	Progressed	Progressed
No. of condensed sperm heads	High	High	High	High	Very low
No. of decondensed sperm heads	High	High	High	High	Very low/not detected

*Preblastodermal cell is referred as the completely closed cell detached from the yolk.

Table 2. Approximate number of condensed sperm heads on the *dorsal side of EG&K stage I–III embryos after penetration

No. of supernumerary sperm	1–10	10–100	100–1000	More than 1000	Total no.
No. of embryos	12	22	22	10	66

*The perivitelline membrane was removed from all embryos and only dorsal surface was focused under the microscope for counting DAPI stained nuclei.

4. Discussion

The finding of this study clearly demonstrated different aspects of sperm penetration and embryo cleavage between birds (chicken) and mammals. There was a unique, radiating progress of preblastoderm furrowing which showed different furrowing status between the dorsal and the ventral surfaces. Interestingly, different status of spermatozoa penetrated into egg preblastoderm was detected and uneven distribution of condensed and decondensed sperm heads were detected in central (furrowing-completed, cleavage-initiated region) and peripheral (furrowing-incomplete, cleavage-progressing region) parts of the preblastoderm. Although it was not certain whether supernumerary sperm move from the center toward the periphery, it was obvious that they were abundant in the periphery than the center. To clarify the exact function of supernumerary sperm on cleavages, what components of sperm contribute to embryos should be identified in further studies. In the yolk on the ventral side, decondensed sperm nuclei were mainly detected, which might imply either the presence of decondensation factor in the yolk or the entry of sperm into the yolk area only through the preblastodermal region. In any case, this is the unique phenomenon in chick embryos, which is not seen in the mammals.

In this study, we used a modified noninvasive collection method (abdominal massage) for retrieving intrauterine EG&K stage embryos, which was originally reported by Eyal-Giladi and Kochav (Eyal-Giladi and Kochav, 1976). Based on this original technique, we provided the detailed information for the classification, which reflected egg shell formation and a compatible comparison was possible between the newly suggested classification and the "conventional" EG&K classification. There has been no classification

reflecting both eggshell formation and embryo development. Combining of EG&K classification with eggshell formation, formation of area pellucida begins from EG&K stage VII, thus this stage was the first lineage differentiation in chicken. Calcium-deposited eggshell was formed from EG&K stage V and eggshell hardening was observed from EG&K stage VII. There seems to be a close correlation between eggshell formation and formation of area pellucida. By employing this modified classification, it will be feasible to identify and to collect embryos at various intrauterine stages.

We found a significant difference in the dynamics of the sperm that had penetrated into oocytes and in early cleavage. Polyspermic fertilization, with large numbers of decondensed or condensed sperm in an oocyte, was observed. Differing from mammals, many unfertilized supernumerary sperm heads were observed in the yolk area, as well as in the cytoplasm. Several sperm heads in the yolk were undergoing decondensation. The sperm tract from the extracellular space into the yolk was unknown, whether it was direct penetration into the yolk or penetration via the cytoplasm. Decondensed sperm may pass through the cytoplasm during the initial stage of egg development.

Asymmetric cleavage was initiated as early as from the first cleavage, which triggered radiation-oriented progress from central to peripheral part. Central cells in a cleaving embryo seemed to divide very rapidly while peripheral cells, including open cells, divided relatively very slowly. The peripheral furrowing could be readily distinguished from the central one by their length and origin. The peripheral cleavage furrows formed from the peripheral edge of embryo, elongated toward the center, and were more easily visible from the ventral side; however, they were not detectable after EG&K stage IV. This furrowing-type cleavage yielded lots of differences compared

with the cleavage of mammalian embryos. In mammals, asymmetric, polarized cleavage signs the initiation of differentiation, while in chick, each part of the preblastoderm being separated was still connected to each other at the ventral side even after initial furrowing. So, it is difficult to simply reflect the knowledge from the mammals and to further justify the signs of initial differentiation.

Preblastodermal cell divides rapidly. Bellairs et al. (Bellairs et al., 1978) stated that the open cells mitotically divide into two daughter cells: one is laterally closed, and the other is open. One daughter nucleus migrates into adjacent yolk, while the other remains *in situ*. This indicates that the possibility of a different division mechanism in open and closed cells. In this study, however, the open cells observed in the peripheral region did not always generate both closed and open daughter cells. They could divide into two open cells as well as both closed and open daughter cells, indicating that the division direction of open and closed cells are not fixed. However, formation of the subgerminal cavity at the center of EG&K stage III embryo (Eyal-Giladi and Kochav, 1976) may be an inducible factor for dividing central cells vertically to create two or more layers.

Polyspermy or supernumerary sperm are not common in mammals, whereas they are consistently found in avian species (Snook et al., 2011). Chick embryos begin normal development after numerous sperm penetrate the oocyte cell membrane, suggesting that supernumerary sperm may be important to ensure karyogamy (Birkhead et al., 1994). Considering the small area of the germinal disc in relation to the entire ovum of the chicken, polyspermy or supernumerary sperm are necessary to ensure fertilization (Snook et al., 2011). Previous reports have shown that low sperm penetration reduces the fertilization rate in chickens (Bramwell et al., 1995; Wishart,

1997). Co-localization of decondensed supernumerary sperm in peripheral small cleavage furrows suggested that decondensation of sperm nuclei is a prerequisite for the short-lived supernumerary sperm-associated peripheral cleavage furrows. We found that decondensed sperm were located mainly on the ventral side of the embryos, specifically underneath the cytoplasm, whereas condensed sperm were located mainly on the dorsal side. This might indicate different role of intracytoplasmic, decondensation factors in development of chicken embryos, compared with mammalian embryos.

CHAPTER 4

Germ Cell Specification in Chicken Revealed by Dynamics of DAZL Gene Expression as a Germplasm during Intrauterine Stages

1. Introduction

Germ cell specification has been explained by two major mechanisms; preformation and induction as described well previously (Extavour and Akam, 2003). In the preformation mode, maternally inherited germplasm containing mRNAs (Subramaniam and Seydoux, 1999; Forrest and Gavis, 2003; Kosaka et al., 2007) and proteins (Hay et al., 1988; Megosh et al., 2006) has a crucial role for germ cell specification in initial developmental stages, as mainly studied in various Drosophila melanogaster (Mahowald, 2001), Caenorhabditis elegans (Hird et al., 1996) and Xenopus laevis (Heasman et al., 1984). In the induction mode, germ cells are induced by signals from neighboring somatic cells during gastrulation, as studied in mouse (Tsang et al., 2001) and Ambystoma mexicanum (Johnson et al., 2001). Taken together, the presence of localized germplasm from the oocyte to the cleavage-stage embryo is one of crucial criteria to distinguish the mode of germ-cell specification.

Chicken primordial germ cells were initially identified in the germinal crescent region of HH stage 4-10 embryos after the formation of primitive streak and thought to originate from the hypoblast based on their location (Swift, 1914). PGCs in the germinal crescent were identified by morphological characteristics such as a large amount of glycogen granules in the cytoplasm and a large cell size compared to the surrounding somatic cells. Because of a large content of glycogen granules, the following studies used the periodic acid Schiff (PAS) staining to distinguish the PGCs (Meyer, 1964).

After that, at late nineteenth, however, Eyal-Giladi and others showed the epiblastic origin of PGCs by the chick-quail chimera study (Eyal-

Giladi et al., 1981). Based on this study, the following works were focused on the induction mode of specification at around EGK stage X (Karagenc et al., 1996; Naito et al., 2001). Also, it is evident that only the central region, not the marginal zone or area opaca of the blastoderm at EGK.X can give rise to PGCs (Ginsburg and Eyal-Giladi, 1987; Naito et al., 2001). It was quite reliable that chicken PGCs arise at around EGK stage X by inductive signals, because there had been no evidence of the presence of germplasm or primordial germ cells during cleavage stages even in quail (Ginsburg et al., 1989). At that time, however, there was no available marker to detect PGCs or the germplasm except PAS staining.

After a chicken vasa homologue (CVH) was isolated, chicken PGCs were traced backwards to initial developmental stages (Tsunekawa et al., 2000). Remarkably, CVH protein is co-localized with spectrin and mitochondrial clouds in the growing oocytes that indicates the presence of germplasm in chicken. Also, CVH protein is localized to cleavage furrows and restricted to only six to eight cells of 300-cell stage embryo as a patch-like structure that is the similar pattern of germplasm inheritance in zebra fish (Raz, 2003).

Above studies suggest strongly that chicken germ cells may be specified by maternally inherited determinant (preformation). To understand mechanisms of germ cell specification in chicken, however, additional studies will be needed by using other reliable germ cell-specific markers and transplantation studies during intrauterine stages.

In the present study, we investigated the expression of chicken deleted in azoospermia-like (cDAZL) gene during intrauterine stages to find

out germ cell specification in chicken. cDAZL mRNA was expressed in the central region during oocyte-to-zygote transition and cleavage stages. cDAZL and CVH also showed similar expression patterns. Furthermore, there was kinetics of cDAZL mRNA expression as a germplasm during germ cell specification. DAZL-expressing PGCs were located elsewhere in the central region regardless of cell layers at EGK.VI-X.

2. Materials and methods

Experimental animals

White Leghorn (WL) hens (54–56 weeks old) were used for the collection of oocytes and intrauterine eggs. We managed chickens according to our standard operation protocol. Relevant experimental procedures for the study were approved by the Institutional Animal Care and Use Committee, Seoul National University before undertaking experiments (SNU-070823-5).

Collection of intrauterine eggs and oocytes from hens

Egg-laying time of WL hens was recorded and intrauterine eggs of EGK stages I to X were harvested by an abdominal massage technique (Eyal-Giladi and Kochav, 1976). Briefly, the abdomen of hens was pushed gently until exposure of the shell gland, and the surface of the shell gland expanded when an egg was located there for eggshell formation. After expansion of the surface of the shell gland, massage was used to move the egg gently toward the cloaca until the intrauterine egg was released. To collect oocytes, three WL hens were sacrificed and the follicles were detached from the ovaries. The oocytes were divided based on the follicles of two different stages; small white follicles (SWFs) and large yellow follicles (LYFs) with less than 0.5 cm and 3.5-4.5 cm diameter, respectively.

Collection of early embryos

White Leghorn eggs were incubated with intermittent rocking at 37–38 °C under 60–70% relative humidity until sample collection. We collected HH stages 4 to 11 for wholemount in situ hybridization (Hamburger and Hamilton, 1992).

Analysis of intrauterine embryos

Intrauterine embryos were separated from the egg using sterilized paper (Chapman et al., 2001) and the shell membrane and albumen were detached from the yolk. A piece of square-type filter paper (Whatman, Maidstone, Kent, UK) with the hole at the center was placed over the germinal disc. After cutting around the paper containing the intrauterine embryo, it was gently turned over and transferred to saline buffer to further remove the yolk and the vitelline membrane for embryo collection (Pannett and Compton, 1924). Collected embryos were fixed with 4% (w/v) paraformaldehyde in 1× phosphate-buffered saline (PBS) and the fixed embryos were classified according to the cleavage stages proposed by Eyal-Giladi and Kochav (Eyal-Giladi and Kochav, 1976). Unfertilized and abnormal embryos were identified by the morphological criteria of cleavage furrows.

Wholemount in situ hybridization

St To make hybridization probes, total RNA from MACS+ PGCs at E6.5 was reverse transcribed, and the cDNA was amplified using cDAZL-specific primers (F: 5' -CGTCAACAACCTGCCAAGGA and R: 5' -TTCTTTGCTCCCCAGGAACC, product size 540 bp) as previously described (Rengaraj et al., 2010). The PCR products of the correct size were

cloned into pGEM-T (Promega). After sequence verification, the recombinant plasmids containing the gene was amplified with T7- and SP6-specific primers (T7:5=TGTAATACGACTCACTATAGGG and SP6: 5=CTATTTAGGTGACACTATAGAAT) to prepare the template for labeling of the hybridization probes. Digoxigenin (DIG)-labeled sense and antisense hybridization probe of cDAZL was transcribed in vitro using a DIG RNA labeling kit (Roche Diagnostics, Indianapolis, IN, USA). For wholemount insitu hybridization, the standard published protocol in chicken was followed (Stern, 1998).

Immunohistochemistry and transmission electron microscopy (TEM)

The collected oocytes and intrauterine embryos were immunostained by wholemount and after paraffin-section, respectively. For immunostaining, oocytes and intrauterine embryos (after deparaffinization for paraffin-sectioned tissues, thickness; 8 μm) were washed three times with PBS and blocked with blocking buffer, which was composed of PBS containing 5% goat serum and 1% bovine serum albumin (BSA) for 1 h at room temperature. Samples were then incubated at 4 C overnight with rabbit anti-cDAZL, anti-CVH or anti-RNA polymerase II CTD repeat antibody (ab5401, abcam, USA). After washing three times with PBS, samples were incubated with secondary antibodies labeled with phycoerythrin or fluorescein isothiocyanate (FITC, Santa Cruz Biotechnology) for 4 h at room temperature. Samples were then mounted with Prolong Gold anti-fade reagent with 4',6-diamidino-2-phenylindole (DAPI, Invitrogen, Carlsbad, CA, USA) and visualized using fluorescence microscopy.

To prepare specimens for transmission electron microscopy (TEM),

samples were dehydrated through a graded ethanol series, embedded in Spurr's resin, and cut on an ultramicrotome (MT-X; RMC, Tucson, AZ, USA). Samples were then stained with 2% uranyl acetate and Reynold's lead citrate for 7 min each and observed under TEM (LIBRA 120; Carl Zeiss) as described in our previous study (Jung et al., 2011)..

3. Results

cDAZL mRNA expression during early germ cell development

During early embryonic development, cDAZL mRNA was expressed specifically in primordial germ cells (PGCs) during their migration as shown in Fig. 1. At HH.4, cDAZL mRNA was expressed in the cells in the germinal crescent region where chicken PGCs are located at HH.4 (Fig. 1A). cDAZL expressing PGCs migrated laterally during HH.4-7 (Fig. 1B and C). Then cDAZL expressing PGCs migrated to near the anterior vitelline veins of the HH.11 embryo (Fig. 1D). Based on the above results, cDAZL can be a good candidate for marker to trace origin of PGCs.

Expression of cDAZL gene and localization of germ-granule during oocyte to zygote transition

To investigate germ-plasm dynamics during oocyte to zygote transition, oocytes from the SWFs and LYFs, embryos of zygote stage and 1st cleavage stage were harvested for wholemount in situ hybridization (Fig. 2). In the oocyte from SWFs, mRNA (Fig. 2A) and protein (Fig. 2B) of cDAZL was expressed in the cytoplasm of oocyte. After further maturation to LYFs, mRNA (Fig. 2C) and protein (Fig. 2D) of cDAZL was strongly localized around the germinal vesicle (GV). Thin sections of the region near the GV of the oocytes from LYFs showed the presence of numerous mitochondria and nonmembranous electron-dense granules (Fig. 3). The electron-dense granules were associated with mitochondrial reticulum (Fig. 3). In the zygote, granular structures of cDAZL mRNA were distributed in the central region of cytoplasm (Fig. 2E). After 1st cleavage started, cDAZL mRNA was also

localized in cleavage furrows (Fig. 2F).

Maternal origin of cDAZL mRNA and zygotic gene activation (ZGA) in early chick embryos

To identify whether initial expression of cDAZL mRNA depends on zygotic transcription or not, unfertilized embryos collected 7h after the oviposition of previous eggs were hybridized with antisense probes for cDAZL. cDAZL mRNA was dispersed in central region as a granular structure like as in fertilized embryos (Fig. S1) that indicated initial localization of cDAZL mRNA was maternally inherited. Also, phosphorylation of RNA polymerase II (p-pol II) in intrauterine embryos showed ZGA starts at least EGK.II-III and progresses from center to periphery (Fig. S2). Taken together, above results indicated cDAZL mRNA is maternally inherited and ZGA in chicken starts at EGK.II-III.

Expression of cDAZL mRNA in intrauterine-stage embryos and the number of PGCs

Localization of germ plasm and formation of PGCs were investigated by tracing expression of cDAZL mRNA (Fig. 4). During initial cleavage stages, cDAZL mRNA was localized in cleavage furrows (Fig. 4A). After embryos further grow with increase of cell layers, cDAZL mRNA was localized in subcellular regions of several central cells from EGK.IV to VI, which indicates the subcellular localization of germ plasm (Fig. 4B and C). Some cDAZL mRNA-containing granules were divided into two daughter cells during mitosis (the sectioned view, Fig. 4B). From EGK.VI to X, cDAZL mRNA was expressed strongly in the cytoplasm of several cells,

PGCs (Fig. 4D-F) indicating the initiation of germline-specific transcription. Some cDAZL-expressing cells revealed mitotic nuclei (the upper sectioned view in Fig. 4E). During intrauterine stages, cells containing germ granules or expressing cDAZL in the cytoplasm were present anywhere among cell layers from the top to the bottom. From initial cleavage stage (EGK.I) to oviposition (EGK.X), expression of cDAZL mRNA in cleavage furrows, in subcellular region and in cytoplasm was restricted to area pellucida where PGCs mainly reside.

The number of PGCs during their specification was counted by whole-section (thickness; 10 μm) of each embryo after wholemount in situ hybridization (Table. 1). The average number of pPGCs and/or PGCs at EGK.V, VI, VII and VIII was 49 ± 5.6 (n=5), 60 ± 18.8 (n=4), 82.2 ± 15.0 (n=5) and 72 ± 11.2 (n=3), respectively.

Expression of germplasm-related protein in intrauterine-stage embryos

To investigate the timing for appearance of primordial germ cells, anti-cDAZL staining was performed with sectioned intrauterine embryos which stages were from EGK.III to X (Fig. 5). At EGK.III, cDAZL protein was localized to cleavage furrows (Fig. 5A), but subcellular localization was not observed. At EGK.V, subcellular localization of cDAZL protein was observed in few centrally-located cells (Fig. 5B). From EGK.VI to X, cDAZL protein was expressed strongly in the cytoplasm of several cells, putative PGCs (Fig. 5C-G). cDAZL expressing PGCs were located in anywhere among cell layers from the top to the bottom. Several cells showed a cluster indicating possible mitosis (Fig. 5C, E and F). CVH, another germplasm-related protein, was co-localized and co-expressed with cDAZL protein (Fig.

6).

Transcriptional status of intrauterine embryos and PGCs

To know whether intrauterine embryos and PGCs are transcriptionally active or inactive, phosphorylation of RNA polymerase II (p-pol II) was investigated. During EGK.IV to X, expression of p-pol II showed a dynamic pattern (Fig. 7). At EGK.IV, central cells were positive for p-pol II, while no phosphorylation was seen in peripheral cells that indicated zygotic genome activation (ZGA) occurs from center to periphery (Fig. 7A). At EGK.V, most of cells are p-pol II-positive (Fig. 7B). However, expression of p-pol II was gradually reduced from upper layers of EGK.VI (Fig. 7C) and lower layers of EGK.VII (Fig. 7D), and most of cells were negative for p-pol II at EGK.VIII (Fig. 7E). p-pol II-positive cells re-increase from EGK.IX (Fig. 7F), and most of cells at EGK.X became positive (Fig. 7G).

Expression of p-pol II in PGCs during EGK.VI to X was also investigated (Fig. 8). The status of p-pol II in PGCs was synchronized with neighboring somatic. At EGK.VI, PGCs were positive for p-pol II, while most of cells including PGCs showed weak expression or negative for p-pol II at EGK.VII (Fig. 8). At EGK.VIII, most of preblastodermal cells including PGCs were negative for p-pol II. At EGK.X, PGCs and other somatic cells reacquired p-pol II (Fig. 8).

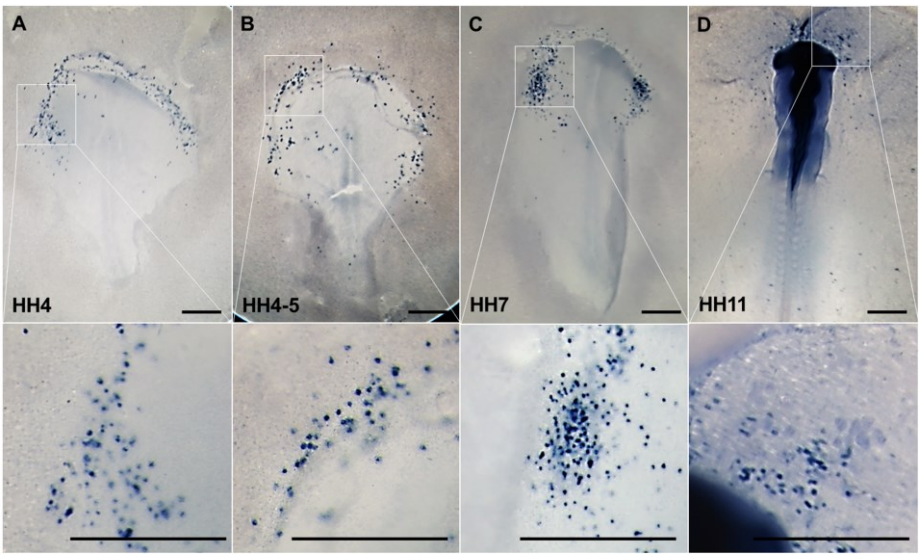

Figure 1. Expression of chicken *deleted in azoospermia-like* (*cDAZL)* mRNA in the embryos from HH stage 4 to stage 11. Whole embryos at stage 4 (A), stage 4-5 (B), stage 7 (C) and stage 11 (D) were hybridized with antisense probes for *cDAZL*. The boxed portions in upper panels are shown at a higher magnification in the bottom panels. Primordial germ cells expressing *cDAZL* mRNA were found in the germinal crescent of the stage 4 embryo and near the anterior vitelline veins of the stage 11 embryos (scale bar = 500 μm).

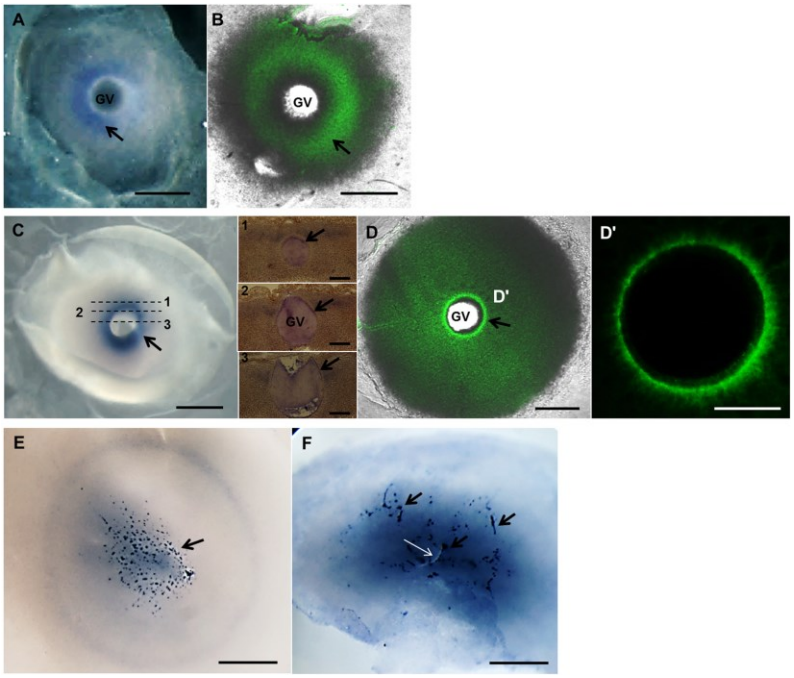

Figure 2. Expression dynamics of mRNA and protein of cDAZL gene during oocyte to zygote transition. In the oocytes from SWFs, *cDAZL* mRNA (A) and cDAZL protein (B) showed cytoplasmic expression (arrows). Scale bar = 500 μm. In the oocytes from LYFs, *cDAZL* mRNA (C) and cDAZL protein (D) was localized around the germinal vesicle (GV) (arrows). Scale bar = 500 μm. Serial sections of the oocyte in (C) (arrows in the panel 1 to 3, scale bar = 100 μm) and the magnified view (D', scale bar = 200 μm) of the GV region in (D) clearly showed the localization around GV. In the zygote (E) and the 1st cleavage-stage embryo (F), *cDAZL* mRNA was dispersed in central region as a granular structure (black arrows, E and F) and some of granules were localized in the cleavage furrow (a white arrow in (F)). Scale bar = 500 μm.

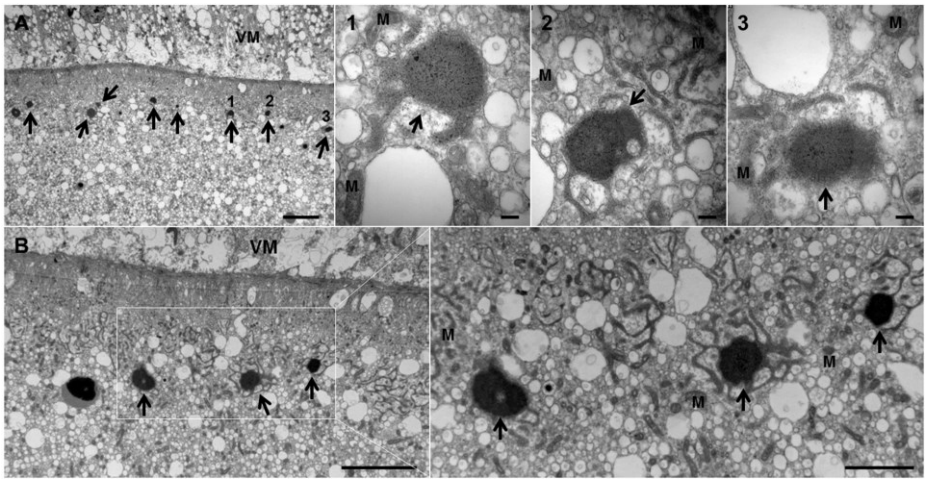

Figure 3. Electron-dense granules associated with numerous mitochondria in the oocyte. Thin sections of the region near the GV of the oocytes from LYFs showed the presence of numerous mitochondria and electron-dense granules (arrows). (A) and (B) showed thin sections of two different oocytes. Scale bars = 5 μm. The right panels of (A) and (B) are the magnified views of the electron-dense granules (number 1 to 3 of A) and the boxed region in (B). Scale bars of magnified views of (A) and (B) are 200 nm and 2 μm, respectively. VM, vitelline membrane; M, mitochondria.

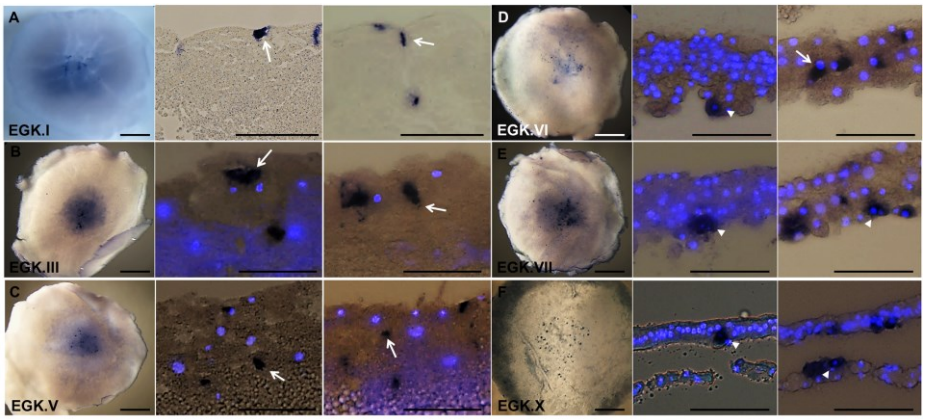

Figure 4. Expression dynamics of cDAZL mRNA on intrauterine embryos. (A) At EGK stage I *cDAZL* mRNA was localized in cleavage furrows as a granular structure (arrow). (B and C) During EGK.III to V, *cDAZL* mRNA was localized in the subcellular region of several centrally located cells (arrows). Some *cDAZL* mRNA-containing granules were divided into two daughter cells during mitosis (the sectioned view of (B), left panel). (D-F) From EGK.VI to X, *cDAZL* mRNA showed diffused expression in the cytoplasm (arrowheads). The right columns for each panel are the sectioned images. Blue spots in sectioned images are DAPI stained nuclei. Scale bars in wholemount and sectioned views are 500 μm and 100 μm, respectively.

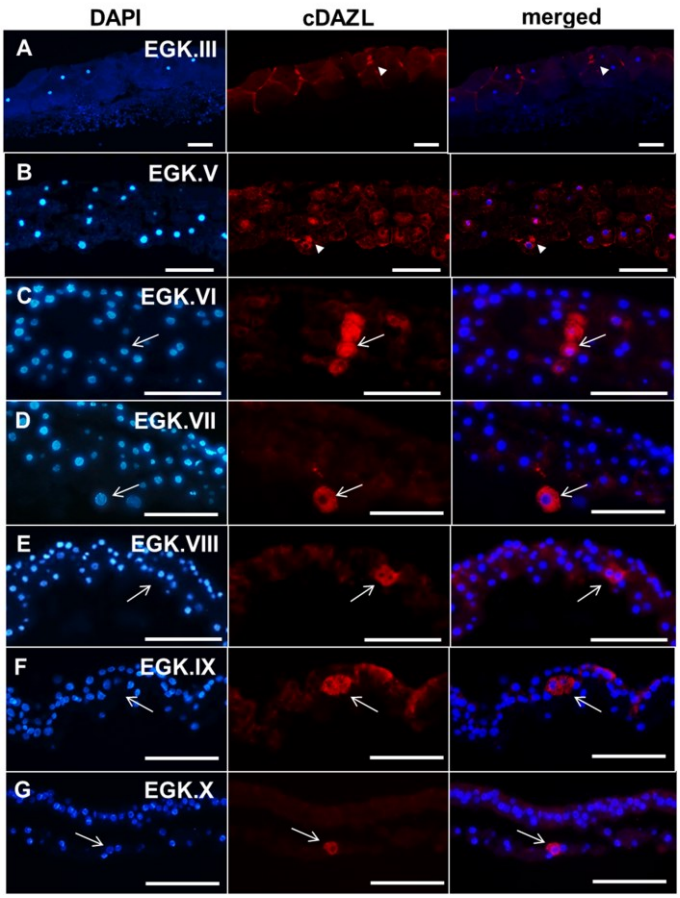

Figure 5. Expression dynamics of cDAZL protein during intrauterine stages. Intrauterine embryos of EGK stage III-X were sectioned and immunostained with anti-cDAZL by PE-conjugated secondary antibody. (A) At EGK.III, cDAZL protein was localized to cleavage furrows (arrowheads). (B) At EGK.V, subcellular localization of cDAZL protein was observed (arrowheads). (C-G) From EGK.VI to X, cDAZL protein was expressed in the cytoplasm of primordial germ cells (arrows). Several cells showed a cluster indicating possible mitosis (C, E and F). Scale bars = 100 μm.

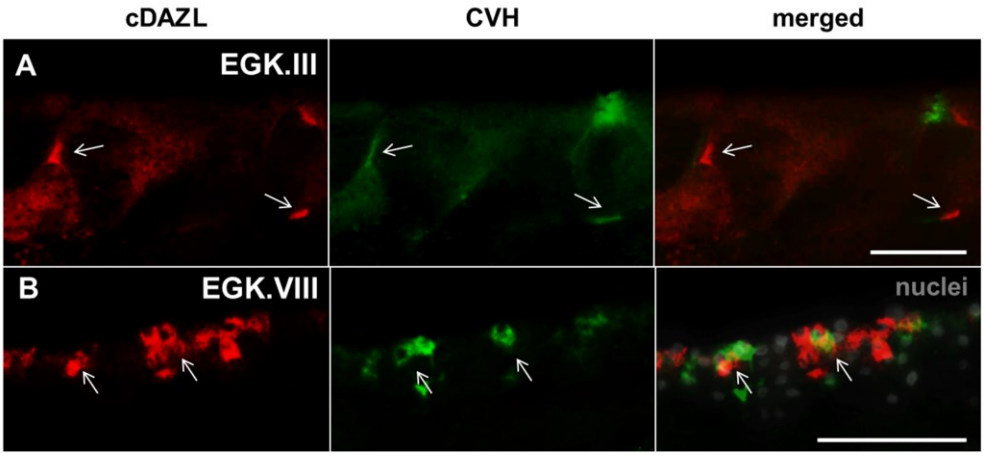

Figure 6. Co-localization of CVH protein and cDAZL protein in a germ granule and PGCs. EGK.III and VIII embryos were serially sectioned and immunostained with anti-CVH and anti-cDAZL. CVH protein and cDAZL protein were co-localized in cleavage furrows as a granule at EGK.III (A, arrows) and in cytoplasm at EGK.VIII (B, arrows). Scale bars = 100 μm.

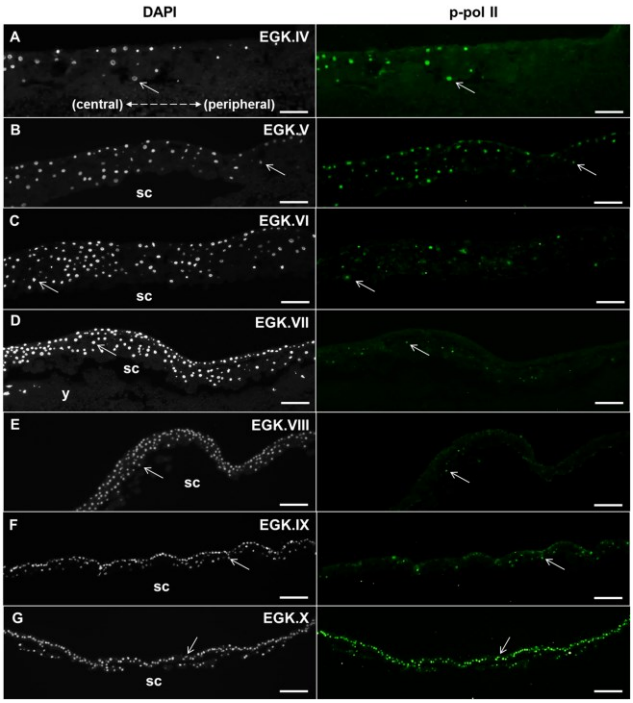

Figure 7. Phosphorylation of RNA polymerase II during intrauterine stages. Intrauterine embryos of EGK stage IV-X were sectioned and immunostained with anti-phosphorylated RNA polymerase II (p-pol II) by FITC- conjugated secondary antibody. (A) At EGK.IV, central cells were positive for p-pol II (arrows), while no phosphorylation was seen in peripheral cells. (B) At EGK.V, most of cells are p-pol II-positive. However, phosphorylation was gradually removed from upper layers of EGK.VI (C) and lower layers of EGK.VII (D), and most of cells were negative at EGK.VIII (E). Phosphorylation restarted at EGK.IX (F) and became positive for most of cells at EGK.X (G). sc, subgerminal cavity; y, yolk region. Scale bars = 100 μm.

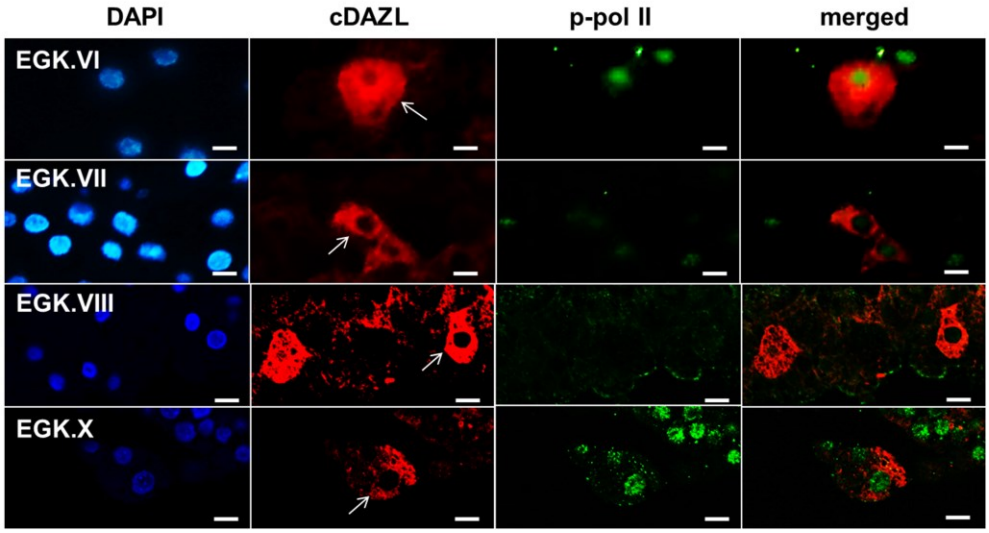

Figure 8. Phosphorylation of RNA polymerase II in PGCs during their specification. Intrauterine embryos of EGK stage VI-X were sectioned and immunostained with anti-cDAZL and anti-phosphorylated RNA polymerase II (p-pol II) by PE- and FITC- conjugated secondary antibody, respectively. At each stage, PGCs showed similar expression pattern of p-pol II with neighboring somatic cells. At EGK.VII, most of cells including PGCs showed weak expression or negative for p-pol II. At EGK.VIII, most of preblastodermal cells including PGCs were negative for p-pol II. The arrows indicate primordial germ cells which were positive for cDAZL. Scale bars = 10 μm.

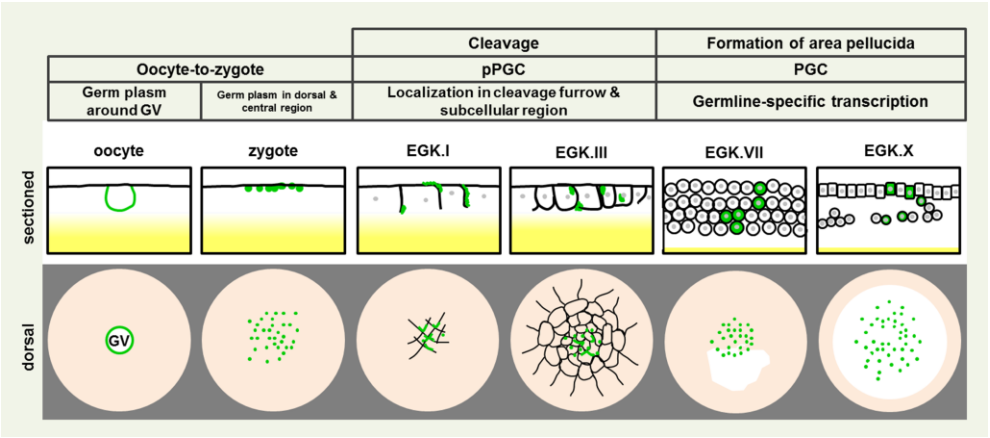

Figure 9. Schematic diagram of germ-plasm dynamics and formation of PGCs in chicken. Green color indicates expression or localization germline-specific gene including cDAZL and CVH. During oocyte-to-zygote transition, germ granules are localized around GV (germinal vesicle) of an oocyte from a pre-ovulatory yellow follicle, and are distributed in the center of zygote. During cleavage stages, germ granules are localized in cleavage furrows at earlier stages and in subcellular region of pPGCs (precursor of PGCs) after formation of preblastodermal cells. After that, germline specific transcription revealed by diffused cytoplasmic expression starts in PGCs (primordial germ cells). PGCs are present randomly in the central region of an embryo regardless of cell layers.

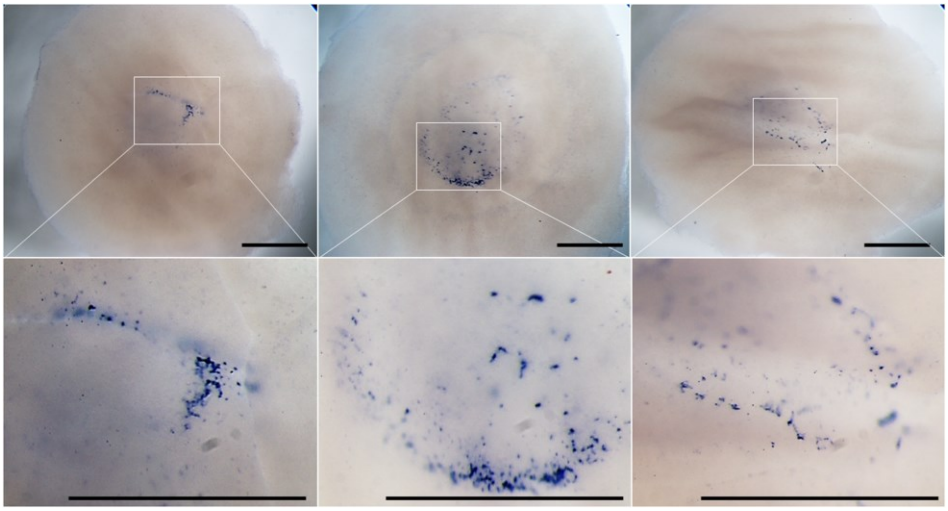

Figure S1. Expression of *cDAZL* mRNA in the unfertilized embryos. Unfertilized embryos were harvested from laying hens without crossing 7h after the oviposition of previous eggs and were hybridized with antisense probes for *cDAZL*. *cDAZL* mRNA was dispersed in central region as a granular structure like as in fertilized embryos. Scale bars = 500 μm.

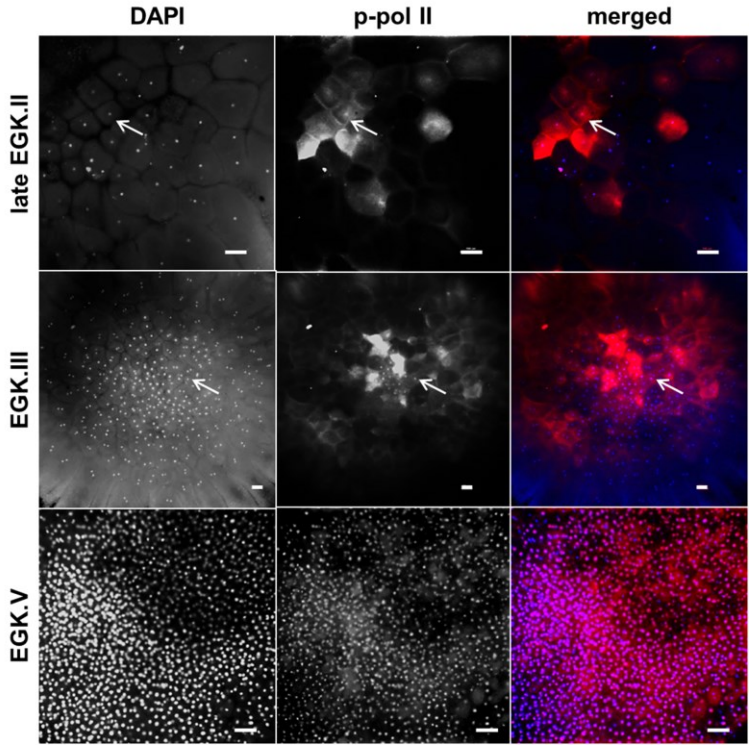

Figure S2. Phosphorylation of RNA polymerase II in intrauterine embryos with a wholemount view. Intrauterine embryos of EGK.II-V were immunostained with anti-phosphorylated RNA polymerase II (p-pol II) by PE- conjugated secondary antibody. At late EGK.II, a few central cells were positive for p-pol II (arrows), while most of cells are p-pol II-positive at EGK.V. Scale bars = 100 μm.

Table 1. Counting of the number of pPGCs and/or PGCs during EGK.V to EGK.VIII

EGK.V		EGK.VI		EGK.VII		EGK.VIII	
embryo No.	No. of cells*	embryo No.	No. of cells	embryo No.	No. of cells	embryo No.	No. of cells
1	31	1	24	1	102	1	94
2	56	2	100	2	128	2	65
3	56	3	32	3	61	3	57
4	61	4	84	4	77		
5	41			5	43		
average	49±5.6	average	60±18.8	average	82.2±15.0	average	72±11.2

*Cells have granular structure (EGK.V-VI) or diffused expression (EGK.VI-VIII) of *cDAZL* mRNA

4. Discussion

During specification of primordial germ cells (PGCs), several germ cell-specific genes are expressed and play a role for maintaining germ cell-competency among various species. They contain nanos, vasa, piwi, dazl and etc (Hay et al., 1988; Johnson et al., 2001; Megosh et al., 2006). DAZL, one of germline-specific genes as a RNA binding protein in diverse species (Xu et al., 2001), has been known to have important roles for meiosis (Eberhart et al., 1996; Saunders et al., 2003) and pluripotency of germ cells (Haston et al., 2009). Also, in chicken, cDAZL is expressed specifically in germ cells from embryonic stages to adult stages (Rengaraj et al., 2010). In the present study, we found that, unlike mammals, cDAZL is also expressed specifically in primordial germ cells during their migration from EGK.X (the pre-streak stage) to HH.11 that indicated the possibility of cDAZL expression before oviposition. Therefore, we selected DAZL gene as the marker for tracing origin of primordial germ cells in chicken.

The presence of germplasm structure and asymmetric localization of germplasm-related genes in the oocytes and cleavage-stage embryo is one of the important criteria to determine the mode of germ cell specification. In flies, only posterior pole cells containing pole plasm that is assembled during oogenesis will give rise to germline cells during whole life (Technau and Camposortega, 1986; Mahowald, 2001). In worms, electron dense granules, called P granules, are localized into the posterior region during zygotic formation, and P4 blastomere harboring the P granules becomes the PGCs (Strome and Wood, 1982; Hird et al., 1996). In chicken, CVH protein is localized into the cortex region of growing oocytes and then into cleavage furrows (Tsunekawa et al., 2000). However, how the germplasm move from

the peripheral cortex in oocytes to the central cleavage furrows in embryos is not identified. We investigated DAZL mRNA expression in the oocyte from preovulatory follicle and found that it was localized in perinuclear region in the center with the approach of ovulation and was maintained during zygote formation. Electron-dense granules with numerous mitochondria were also present near the GV of oocyte. In addition, expression of cDAZL mRNA in unfertilized embryos and p-pol II during intrauterine stages in our results indicated that cDAZL mRNA is maternally inherited rather than zygotic transcription. Also, cDAZL mRNA expression in the central region was maintained during cleavage progress. Also, cDAZL protein showed a similar expression pattern during all stages we investigated. Taken together, in chicken, the site for asymmetric localization of germplasm seems to be central region of embryo like as the posterior region in flies and worms (Hird et al., 1996; Mahowald, 2001). This interpretation is in accordance with previous studies that showed central position of PGCs near EGK.X (Ginsburg and Eyal-Giladi, 1987; Naito et al., 2001). Also, when comparing CVH expression in the previous study (Tsunekawa et al., 2000) and DAZL gene expression in our study, it seems that CVH and DAZL are co-localized together in germplasm as studied for their binding activity (Reynolds et al., 2005). Besides, other components of germplasm in chicken should be investigated to know their regulatory mechanisms.

We found that there was kinetics of DAZL gene expression during cleavage stages. During intrauterine embryo development, DAZL was localized in cleavage furrows during initial cleavage progression (EGK.I-III), localized in subcellular region during further cleavage (EGK.IV-VI) and finally diffused in cytoplasm after EGK.VI-VII. We also found similar expression pattern of CVH after EGK.VII. The diffused expression of DAZL in cytoplasm was thought to be the initiation of germline-specific

transcription. Therefore, considering their mitotic feature with clustering in our results, we proposed that PGCs in chicken arise from at EGK.VI-VII which are derived from presumptive PGCs (pPGC) containing the germplasm localized in subcellular region based on the nomenclature of Nieuwkoop and Sutasurya (Nieuwkoop and Sutasurya, 1979). Also, the diffused expression of DAZL in cytoplasm was thought to be the initiation of germline-specific transcription. Germline-specific transcription during or after germ cell specification is closely related with transcriptional repression in germ cells (Nakamura and Seydoux, 2008). Germline-specific transcription starts after specification in C. elegans (Seydoux and Fire, 1994) and Drosophila (Zalokar, 1976), while it is correlated with specification in mouse (Saitou et al., 2002). In our results, phosphorylation of RNA polymerase II in PGCs during their specification was synchronized with other somatic cells. Our results indicated that global transcriptional repression in PGCs during specification as in C. elegans and Drosophila is not a common mechanism in chicken. Thus, how germline competency is maintained during specification will be studied by investigation of other genes to repress selectively somatic genes in germ cells (e.g. Blimp1 in mouse) in the further study.

Previous studies reported that avian germ cells originate from the epiblast, not from the hypoblast (Eyal-Giladi et al., 1981; Ginsburg and Eyal-Giladi, 1986). At EGK.X, area pellucida has the epiblast in upper layer and the primary hypoblast in lower layer, and the primary hypoblast was thought to be derived by poly-ingression from the epiblast (Weinberger et al., 1984). In our results, however, PGCs were consistently found not only in the most upper layer but also in the lower layers at least from EGK.VI-VII (5-6 cell-layer thickness) until EGK.X (1-2 cell-layer thickness). Also, serial sections from EGK.VII to EGK.X in our results showed that initial segregation of the primary hypoblast may already start at EGK.VII. In this view, at EGK.VII, the

most upper layers seem to be future epiblast and the lower layers seem to by future hypoblast. Therefore, we thought that PGCs be already present not only in the epiblast but also in the hypoblast in pre-streak stage embryos. For better understanding, investigation for expression pattern of lineage-specific genes during intrauterine embryo development is needed.

Conclusively, we reported that origin of PGCs and germ-plasm dynamics during specification in chicken (Fig. 8). Also, DAZL is a great maker to trace germ cells in chicken being expressed specifically in germ cells from cleavage stages to adult stages. DAZL seem to be one of germplasm components as well as CVH, and PGCs arise at least EGK.VI-VII with initiation of germline-specific transcription in chicken. To know the exact function of DAZL during germ cell specification, loss of function studies will be needed in the further study.

CHAPTER 5

Compensatory proliferation of endogenous chicken primordial germ cells after elimination by busulfan treatment

1. Introduction

The continuous maintenance of future generation in living organisms is preserved by germ cell development. Thus, germ cell research is important to advance infertility treatments and perform developmental studies. Elimination of endogenous germ cells has been widely used in germ cell transplantation studies (for clinical purposes) and germline chimera production (for research purposes). Several methods including gamma ray irradiation, x-ray irradiation (Van Buul et al., 1995; Campion et al., 2010; Park et al., 2010), and busulfan administration (Song et al., 2005; Lee et al., 2006; Nakamura et al., 2010) to eliminate endogenous germ cells in different vertebrate species have been developed. These methods primarily induce DNA damage in target cells, resulting in loss of all cellular mechanisms and ultimately cell destruction. Busulfan is an alkylating agent that can induce target cell apoptosis when administrated into cells or tissues. Until recently, busulfan treatment was the preferred method of eliminating germ cells. Although busulfan administration can induce side effects including lethality, sterility and teratogenicity (Bishop and Wassom, 1986), the majority of studies have applied busulfan to eliminate germ cells in mouse and rat testis because of its relatively higher cytotoxicity to target cells. After busulfan administration, testicular germ cells undergo apoptosis; however, small population of spermatogonial stem cells (SSCs) survive in mice (Choi et al., 2004). These surviving SSCs may be involved in restoration of the germ cell population after reduction or withdrawal of busulfan toxicity (Zohni et al., 2012).

Primordial germ cells (PGCs) are the precursors of germ cells in most vertebrates and play an important role in early embryonic germ cells

(Han, 2009). Elimination of PGCs by busulfan administration can be performed in early chicken embryos because isolation and manipulation of PGCs from these embryos is simple compared to other vertebrate embryos. In chickens, PGCs originate in the epiblast and migrate through the hypoblast and blood to reach embryonic gonads. Busulfan administrated into chicken eggs at Eyal-Giladi and Kochav (EG&K) stage X (Eyal-Giladi and Kochav, 1976) successfully eliminated all endogenous PGCs in the embryos. After busulfan treatment, donor PGCs injected into the embryos migrated and colonized on the recipient gonads. The proportion of donor-derived offspring was also increased significantly (Nakamura et al., 2008; Nakamura et al., 2010). However, little about the cellular responses of PGCs after busulfan treatment is known. In the present study, we conducted flow cytometric analysis to evaluate changes in the PGC proportion and cell cycle status after busulfan treatment in chickens.

2. Materials and methods

Experimental animal care

The care and experimental use of chickens were approved by the Institute of Laboratory Animal Resources, Seoul National University (SNU-070823-5). White Leghorn (WL) chickens were maintained according to a standard management program at the University Animal Farm, Seoul National University, Korea. The procedures for animal management, reproduction, and embryo manipulation adhered to the standard operating protocols of our laboratory.

Survival and hatching rates

To measure survival rates, egg candling was performed for each egg during the observation period. Properly developing eggs were identified based on the clear demarcation of light and dark side within the egg and the formation of a network of blood vessels reaching toward the air space. Unfertilized eggs at day 3 were removed from the data and hatching of the eggs occurred at approximately day 21.

Busulfan emulsification

Emulsification of busulfan and injection into chicken embryos was performed as described by Nakamura et al. (2010), with minor modifications (Nakamura et al., 2010). A schematic diagram of busulfan emulsification and injection into eggs is shown in Figure 1. Approximately 40 mg of busulfan

(Sigma-Aldrich, St. Louis, MO, USA) were dissolved in 1 ml of N,N-dimethyl formamide (Merck, Darmstadt, Germany) and diluted 10-fold in phosphate-buffered saline (PBS). For emulsification, an internal pressure micro kit (IMK-20; MCtech Siheung, Korea) was used as a dispersion-emulsifying system with a tube-shaped Shirasu porous glass (SPG; pore diameter, 10 μm) membrane. The dispersed phase inside the SPG membrane was filled with busulfan-solubilized solution, and the continuous phase outside of the SPG membrane was filled with the same volume of sesame oil (Santa Cruz Biotechnology, Inc. Santa Cruz, CA, USA) with 1% polyglycerol polyricinoleate (PGPR90, Danisco, Denmark) (Figure 2). The internal pressure was injected using nitrogen gas while stirring the continuous phase with a rotator. The final concentration of busulfan in the emulsion was 2 μg / μl in sesame oil containing 1% PGPR90. To optimize the concentration of PGPR90, particle size uniformity and color of the emulsified solution with different concentrations of PGPR90 were observed at time 0 and 1 day after emulsification. Newly laid WL eggs at EG&K stage X were placed horizontally 1 h before injection. The optimal dose of busulfan was determined based on Nakamura et al. (2010) (Nakamura et al., 2010). A small hole was made at the sharp end of eggs to avoid air cell damage and 50 μl of busulfan emulsion (100 μg of busulfan) were injected into the yolk under the blastoderm through a small hole using a sharp needle. After injection, the hole was sealed and the eggs were incubated at 37°C with 50-60% relative humidity until the gonads were isolated at embryonic day 5.5, 7, 9 and 15.

EdU incorporation

To examine the proliferation activity of germ cells, approximately 10 μl of 10 mM EdU in PBS was injected into the extra-embryonic blood vessels 4 h before embryonic day 9. After injection, the eggs were sealed with

Parafilm and incubated until the completion of embryonic day 9.

Immunohistochemistry

After 5.5- and 9-day embryos treated with busulfan at stage X were collected, the abdomen of the embryos was carefully dissected under a stereomicroscope and the gonads were collected with sharp tweezers (Park et al., 2003). Whole gonads were then cryosectioned (thickness; 10 μm) or paraffin-sectioned (thickness; 6 μm) and stored for immunostaining. For immunostaining, gonadal sections (after deparaffinization for paraffin-sectioned tissues) were washed three times with PBS and blocked with blocking buffer, which was composed of PBS containing 5% goat serum and 1% bovine serum albumin (BSA) for 1 h at room temperature. Sections were then incubated at 4°C overnight with rabbit anti-cVASA (chicken VASA homology) antibody to detect germ cells. After washing three times with PBS, sections were incubated with secondary antibodies labeled with phycoerythrin or fluorescein isothiocyanate (FITC, Santa Cruz Biotechnology) for 4 h at room temperature. To detect incorporated EdU, sections were further stained for Click-iT detection with Alex Fluor 594 according to the manufacturer's instructions. Sections were then mounted with Prolong Gold anti-fade reagent with 4',6-diamidino-2-phenylindole (DAPI, Invitrogen, Carlsbad, CA, USA) and visualized using fluorescence microscopy.

Flow cytometry

For flow cytometry, whole gonads of 5.5-, 7-, 9- and 15-day busulfan-treated embryos were disassociated by gentle pipetting in 0.05% (v/v) trypsin solution supplemented with 0.53 mM ethylenediaminetetraacetic

acid (EDTA), fixed with 4% paraformaldehyde and permeabilized. Cells were then suspended in PBS containing 1% BSA and strained through a cell strainer (40 μm, BD Falcon; Becton Dickinson, NJ, USA). Cell aliquots were incubated in 500 μl of 1% BSA in PBS containing primary antibodies (chicken VASA) on ice for 30 min. After washing with PBS, cells were incubated in FITC-conjugated secondary antibodies on ice for another 20 min. For cell cycle analysis, RNase treatment and propidium iodide (PI) staining were performed. Flow cytometry was performed on a FACSAria III (Becton Dickinson). All subsequent analyses were performed using FlowJo software (Tree Star; Ashland, OR, USA) and Modifit LT cell cycle analysis software (Verity Software House, Topsham, ME, USA).

Statistical analysis

Statistical analysis was performed using Student's t-test in the SAS version 9.3 software (SAS Institute, Cary, NC, USA). The significance of differences between control and treatment groups were analyzed using the general linear model (PROC-GLM) in the SAS software. Differences between treatments were considered significant at $P < 0.05$.

3. Results

Emulsification conditions for busulfan with PGPR90 by IMK-20

For efficient emulsification of busulfan, PGPR90 was used as an emulsifier. The particle size uniformity was observed under the microscope to confirm the effect of 0.0–10.0% PGPR90 on emulsification (Figure 2A). Emulsification did not occur with 0% PGPR90, whereas very low-level emulsification was observed with 0.1% of PGPR90. With 1%, 5% and 10% PGPR90, the particle size uniformity was maintained even after 24 h (Figure 2B).

Survival and hatching rate of the chicken embryos after busulfan treatment

To evaluate teratogenic effects of busulfan treatment, we determined the survival and hatching rates during embryonic development. The survival rates of the busulfan treatment group were significantly lower than those of the untreated control group during development. The survival rates of the control and busulfan-treated groups showed no differences at day 3 but were significantly lower in the busulfan-treated group after 7 days of incubation ($p < 0.05$). Upon hatching, the survival rates of the two groups were significantly different ($p < 0.01$) (Table 1). Mean hatching rates of the untreated control and busulfan treatment groups were 84.47 ± 1.49% (n = 3, total events = 71) and 61.85 ± 2.59% (n = 3, total events = 144), respectively.

Elimination and restoration of PGCs after busulfan treatment

Depletion of PGCs after busulfan treatment was investigated by immunohistochemistry. Whole gonads were collected at embryonic days 5.5 and 9 in both sexes and cryosectioned prior to immunostaining. To identify germ cells, an anti-VASA primary antibody and PE-conjugated secondary antibody were used. At day 5.5, numerous VASA-positive PGCs were dispersed in the gonads of the male and female control group (Figure 3). However, the number of VASA-positive PGCs was greatly decreased in male and female gonads of the busulfan-treated group. At day 9, VASA-positive germ cells were dispersed throughout the male gonads and dispersed in the cortex region of female gonads. In the busulfan-treated group, few VASA-positive germ cells were observed in male and female gonads. Furthermore, the number of VASA-positive germ cells in busulfan-treated female gonads at day 9 was slightly higher than that of busulfan-treated female gonads at day 5.5 (Figure 3).

To examine the proportion of PGCs after busulfan treatment, VASA-positive cells in the embryonic gonads were analyzed by flow cytometry. The mean proportions of PGCs normalized to control PGCs in whole gonads at days 5.5, 7, 9 and 15 are shown in Figure 4. In day 5.5 embryonic gonads, the proportion of PGCs was decreased significantly after busulfan treatment (male; 24%, female; 8%, normalized to control, n = 3). In day 7, 9 and 15 embryonic gonads, the proportion of PGCs was also decreased significantly after busulfan treatment (male; 23%, 60% and 71%, female; 67%, 60% and 65%, respectively, normalized to control, n = 3). The rates of VASA-positive PGCs in all busulfan-treated groups regardless of sex or developmental stage were significantly lower than those in the control groups ($p < 0.001$) (Figure 4). However, the proportion of PGCs in the busulfan-treatment group was significantly increased at embryonic day 9 in male and at embryonic day 7 in female compared to embryonic day 5.5 (Figure 4). Consistent with this germ

cell recovery phenomenon, chickens in the busulfan-treated group produced functional sperms or eggs when they reached sexual maturity (n = 5 for male and n = 3 for female).Cell cycle regulation after busulfan treatment

To examine changes in the cell cycle of PGCs during the recovery period after busulfan treatment, the cell cycle in VASA-positive PGCs of day 9 gonads was evaluated by flow cytometry using PI staining. Representative and replicate cell cycle results in the PGCs of day 9 gonads after busulfan treatment are shown in Figure 5A and 5B, respectively. In both males and females, the proportion of PGCs in the quiescent phase (G0/G1) of the busulfan treatment group was significantly decreased compared to the control group (male; 74.03 ± 0.68% to 68.65 ± 1.27%, female; 63.13 ± 1.03% to 58.17 ± 0.61%, n = 3). In contrast, the proportion of PGCs in the proliferative phase (S/G2/M) of the busulfan-treatment group was significantly increased compared to the control group (male; 25.91 ± 0.68% to 31.35 ± 1.27%, female; 36.87 ± 1.03% to 41.83 ± 0.61%, n = 3). The proportion of PGCs in SubG1 did not show significant changes between two groups in both males and females.

Proliferation of restored PGCs after busulfan treatment

To examine proliferation activity of the restored PGCs in the busulfan treated group, EdU incorporated 9-day-old embryonic gonads were isolated and immunostained with anti-VASA and EdU. Results showed that EdU-incorporated cell nuclei in the male and female gonads of busulfan treated groups were increased when compared to control groups (Figure 6A). Furthermore, we investigated the number of proliferating germ cells by counting the number of EdU-positive cells among VASA positive cells. The

number of proliferating germ cells increased by about 15% in busulfan treated male gonads compared to the control. Similarly, the number of proliferating cells increased by about 30% in busulfan treated female gonads (Figure 6B).

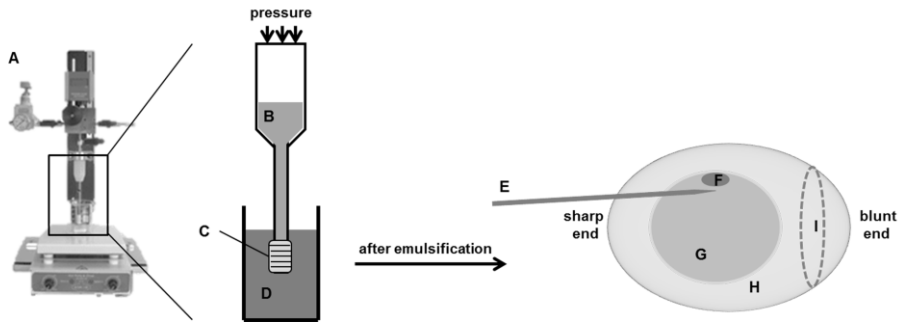

Figure 1. Schematic diagram of the methods for busulfan emulsification and injection into eggs. (A) Internal pressure-type micro kit (IMK-20), (B) Busulfan solubilized in 10% N,N-dimethylformamide in phosphate-buffered saline, (C) Hydrophobic membrane with 10-μm pore diameter, (D) Sesame oil with polyglycerol polyricinoleate (PGPR90), (E) Sharp needle, (F) Blastoderm, (G) Egg yolk, (H) Egg white, and (I) Air space.

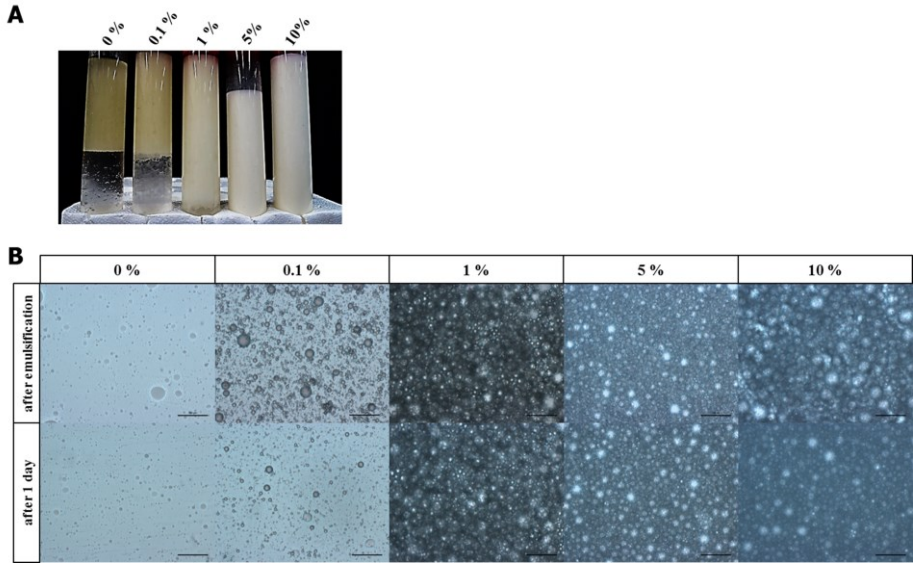

Figure 2. Increase in particle size uniformity according to polyglycerol polyricinoleate (PGPR90) concentration. (A) Solution feature emulsified with sesame oil containing various PGPR90 concentrations. (B) Particle size uniformity after emulsification and after 1 day (scale bar = 100 μm).

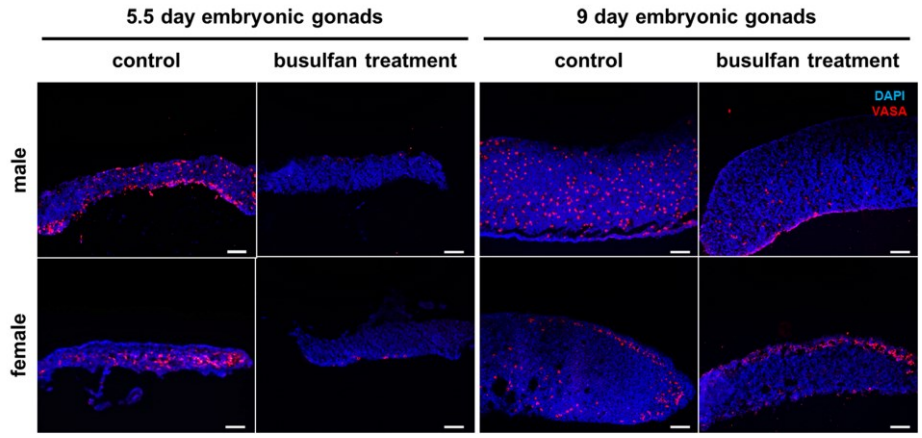

Figure 3. Elimination and restoration of endogenous PGCs in embryonic gonads by busulfan treatment at stage X. Immunostaining was performed to detect germ cells in 5.5- and 9-day-old embryonic gonads using an anti-VASA primary antibody and PE-conjugated secondary antibody. Scale bar = 100 μm.

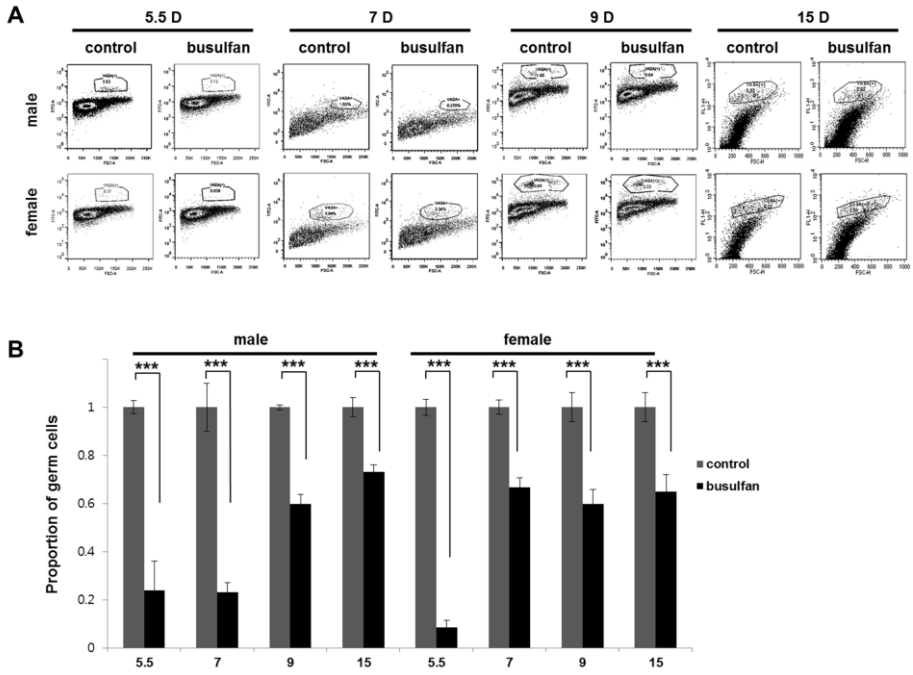

Figure 4. Proportion of PGCs in the embryonic gonads after busulfan treatment at stage X. (A) Representative flow cytometry dot plots of 5.5-, 7-, 9- and 15-day-old embryonic gonadal cells labeled with anti-VASA. (B) Proportion of PGCs in the embryonic gonads of the busulfan treated group. Data were normalized to the proportion of PGCs in the control. Bars indicate SEM of triplicate analyses. ***P < 0.001, significant difference compared to the control.

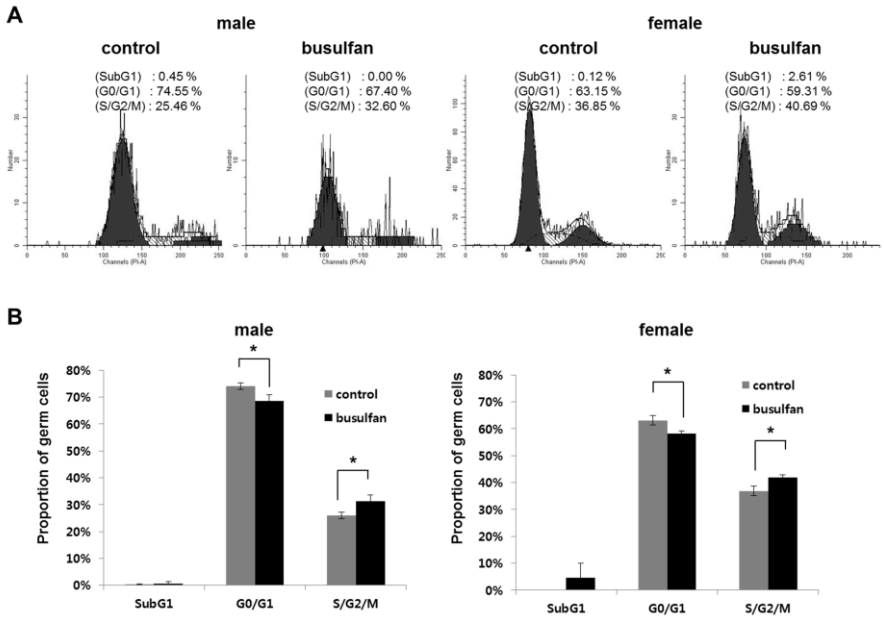

Figure 5. Cell cycle analysis in the PGCs of 9-day-old embryonic gonads after busulfan treatment at stage X. VASA-positive cell populations in embryonic gonads derived from flow cytometry were evaluated in terms of cell cycle phase. (A) Results of representative cell cycle evaluations in males and females. (B) Results of replicate cell cycle evaluations in males and females. Bars represent the SEM of triplicate analyses. *P < 0.05, significant difference compared to the control.

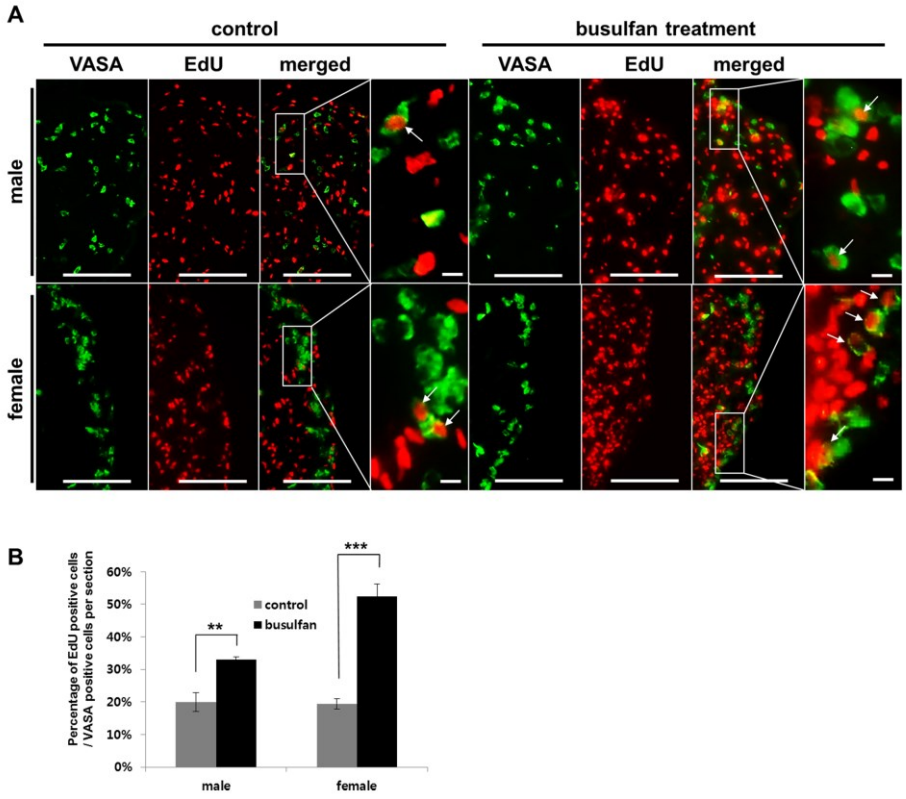

Figure 6. Proliferation of PGCs in 9-day-old embryonic gonads after busulfan treatment at stage X. To detect proliferating PGCs, embryonic gonads were isolated at 9-days (4 h after EdU incorporation) and sectioned for staining with anti-VASA and EdU (A). Scale bars = 100 μm (common views) and 10 μm (magnified views). (B) Percentage of EdU positive cells among VASA-positive cells in the embryonic gonads. Four embryos were evaluated for both sexes. **P < 0.01 and ***P < 0.001, significant difference compared to the control

Table 1. Survival and hatching rates of chicken embryos after busulfan treatment.

Dose (μg)	No. of embryos	Survival rates of embryos on incubation day (%)						Hatched (%)
		3 day	7 day	10 day	14 day	17 day	20 day	
Untreated controls (0)	71	94.47±1.08	92.96±1.41	89.93±4.17	88.64±3.99	88.64±3.99	85.91±2.81	84.47±1.49
Busulfan treated (100)	144	87.03±3.16	77.65±3.36	69.75±4.93	68.39±5.31	68.39±5.31	67.65±5.01	61.85±2.59
P value		0.0902	0.0136	0.0354	0.0381	0.0381	0.0336	0.0016

4. Discussion

To eliminate endogenous PGCs in chickens by busulfan treatment, a sustained-release emulsion of busulfan using an SPG pumping connector was used in a previous study (Nakamura et al., 2010). Here, we modified the emulsion methods using an internal pressure micro kit with a tube-shaped SPG membrane and PGPR90. Using this method, we could simplify the preparation of solubilized busulfan and obtain an increased hatching rate (61.85%) in the busulfan-treatment group when compared to previous studies that used the same busulfan dose (Nakamura et al., 2010).

Busulfan, an alkylating agent, has been used for clinical studies of chronic myelogenous leukemia and bone marrow transplantation (Down and Ploemacher, 1993; Buggia et al., 1994). Generally, busulfan targets slowly proliferating and non-proliferating cells. The mechanism of action of busulfan has been identified as DNA alkylation leading to DNA–DNA cross-linking (Iwamoto et al., 2004), which causes cell death and/or cellular senescence through the ERK and p38 pathways. Busulfan also functions as a mitogen-activated protein kinase (Probin et al., 2007). Conservation of antimitotic pathway across various cell types remains unclear. Busulfan can specifically target and kill germ cells in embryonic gonads or testes leading to the depletion of endogenous germ cells. Therefore, PGCs which are a precursor of gametes may be a major target for the germ cell depletion and sterilization. To target PGCs, busulfan should be administrated at very early embryonic stages during which PGCs are formed. There are about 30 PGCs in the blastoderm of a fertilized hen egg (Tsunekawa et al., 2000). Therefore, busulfan has been used to produce PGC-mediated germline chimeras by direct injection into blastoderm of fertilized eggs in chickens (Song et al., 2005;

Nakamura et al., 2008; Nakamura et al., 2010). When injected into EG&K stage X, busulfan efficiently removed endogenous PGCs. To our knowledge, restoration of endogenous PGCs after busulfan treatment has not been reported to date.

In both sexes, the relative PGC ratios of the busulfan-treated group to the normal embryos at 9 days were markedly higher than that those at day 5.5. Also, sexually mature male and female chickens treated with busulfan at stage X were able to produce functional sperms or eggs. These results indicated that germ cells were recovered from the cytotoxic effects of busulfan during development. Thus, we hypothesized the existence of a compensation mechanism to recover from busulfan toxicity in PGCs. To confirm the increase in PGCs after busulfan treatment, we conducted flow cytometry to enumerate the increase in PGC number. The number of PGCs in the busulfan-treatment group recovered to ~60% that of the control group. This suggested the existence of compensation and/or recovery mechanism in response to cytotoxic damage in PGCs, which is one of the characteristics of stem cells. A strong defensive mechanism against cytotoxic damage has been demonstrated in various stem cells, including SSCs and embryonic stem cells (Choi et al., 2004; Saretzki et al., 2008). To determine whether this compensation is caused by changes in the cell cycle, we conducted flow cytometry with PI staining to discriminate non-proliferating and proliferating PGCs after busulfan treatment. The decrease in the proportion of G0/G1 phase and increase that of S/G2/M phase PGCs after busulfan treatment indicated that the cell cycle status of some PGC populations changed from quiescent (G0) to proliferative (S/G2/M) phases. This change in cell cycle status was further confirmed by the proliferation assay with EdU incorporation. We found that the proportion of EdU positive cells among VASA positive cells was significantly higher in the busulfan treated group.

Our results could be interpreted in two ways: (1) A subpopulation of PGCs with stem cell characteristics proliferated, while the majority of PGCs underwent apoptosis after busulfan treatment; or (2) proliferation of existing PGCs after busulfan treatment suggested that PGCs possess defensive mechanisms against cytotoxicity. Consistent with (1), there exists a side-population (SP) of PGCs in mice (Scaldaferri et al., 2011), which have a greater ability to develop into pluripotent stem cells (Matsui and Tokitake, 2009). In addition, SP cells that differentiated from PGCs were enriched in spermatogonia of developing mice testes (Lassalle et al., 2004). However, the relationship between subpopulations of PGCs and proliferating PGCs after cytotoxic effects was not investigated and little is known about the existence of SP cells in chicken germ cells. Consistent with (2), conserved expression of several pluripotency-related genes (Yeom et al., 1996; Kerr et al., 2008) and microRNAs (Lee et al., 2011) were identified in PGCs. PGCs have the potential to transform into pluripotent embryonic germ cells (Labosky et al., 1994; Park et al., 2003), which indicated that PGCs maintain their undifferentiated state and stem cell attributes in their genetic status. To understand the compensation and/or restoration mechanisms of chicken PGCs, it is necessary to characterize the proliferating PGC subpopulation in busulfan-treated chicken gonads.

Our data suggest that endogenous PGCs can recover from the cytotoxic effects of busulfan. The cell cycle status of PGCs shifted to a lower proportion in the G0/G1 phase and a higher proportion in the S/G2/M phase after busulfan treatment, which indicates that the recovery of PGCs is strongly associated with the cell cycle transition. Our data increase our understanding of PGCs and provide an important basis for germ cell plantation studies.

CHAPTER 7

GENERAL DISCUSSION

The fundamental question in developmental biology is where and when cells originate and how their fates are controlled. A large portion of development of the researches in life science, biotechnology and medical science are based on the research on cell-fate programs. For example, recent research development of embryonic stem cells (ESCs) and induced pluripotent stem cells (iPSCs) and their contribution toward human disease treatment is derived from the fundamental knowledge of developmental biology and is the application of artificial cell-fate control. Germ cells are the only cell population in the body that can transfer genetic information across generations. Thus, their origin, regulatory mechanisms and potential have been one of major interests in this filed. Avian species is located in the important position for evolutional biology and has been used for research model for germ cell biology and application. Therefore, through studying the origin and potential of avian PGCs, we expect to answer unsolved problems in developmental biology and for future applications

The finding of the first study clearly demonstrated different aspects of sperm penetration and embryo cleavage between birds (chicken) and mammals. There was a unique, radiating progress of preblastoderm furrowing which showed different furrowing status between the dorsal and the ventral surfaces. Interestingly, different status of spermatozoa penetrated into egg preblastoderm was detected and uneven distribution of condensed and decondensed sperm heads were detected in central and peripheral parts of the preblastoderm. Although it was not certain whether supernumerary sperm move from the center toward the periphery, it was obvious that they were abundant in the periphery than the center. To clarify the exact function of supernumerary sperm on cleavages, what components of sperm contribute to embryos should be identified in further studies. Through the first study, we could

figure out developmental characteristics and structural dynamics during intrauterine chick-embryo development, that help us to study the origin of PGCs.

During specification of primordial germ cells (PGCs), several germ cell-specific genes are expressed and play a role for maintaining germ cell-competency among various species. DAZL, one of germline-specific genes as a RNA binding protein in diverse species (Xu et al., 2001), has been known to have important roles for meiosis (Eberhart et al., 1996; Saunders et al., 2003) and pluripotency of germ cells (Haston et al., 2009). Also, in chicken, cDAZL is expressed specifically in germ cells from embryonic stages to adult stages (Rengaraj et al., 2010). In the present study, we found that, unlike mammals, cDAZL is also expressed specifically in primordial germ cells during their migration from EGK.X (the pre-streak stage) to HH.11 that indicated the possibility of cDAZL expression before oviposition. Therefore, we selected DAZL gene as the marker for tracing origin of primordial germ cells in chicken.

The presence of germplasm structure and asymmetric localization of germplasm-related genes in the oocytes and cleavage-stage embryo is one of the important criteria to determine the mode of germ cell specification. In chicken, CVH protein is localized into the cortex region of growing oocytes and then into cleavage furrows (Tsunekawa et al., 2000). However, how the germplasm move from the peripheral cortex in oocytes to the central cleavage furrows in embryos is not identified. We investigated DAZL mRNA expression in the oocyte from preovulatory follicle and found that it was localized in perinuclear region in the center with the approach of ovulation and was maintained during zygote formation. Also, cDAZL mRNA expression in the central

region was maintained during cleavage progress. Also, cDAZL protein showed a similar expression pattern during all stages we investigated. Taken together, in chicken, the site for asymmetric localization of germplasm seems to be central region of embryo like as the posterior region in flies and worms (Hird et al., 1996; Mahowald, 2001). This interpretation is in accordance with previous studies that showed central position of PGCs near EGK.X (Ginsburg and Eyal-Giladi, 1987; Naito et al., 2001). Also, when comparing CVH expression in the previous study (Tsunekawa et al., 2000) and DAZL gene expression in our study, it seems that CVH and DAZL may be co-localized together in germplasm as studied for their binding activity (Reynolds et al., 2005). Besides, other components of germplasm in chicken should be investigated to know their regulatory mechanisms.

We found that there was kinetics of DAZL gene expression during cleavage stages. During intrauterine embryo development, DAZL was localized in cleavage furrows during initial cleavage progression (EGK.I-III), localized in subcellular region during further cleavage (EGK.IV-VI) and finally diffused in cytoplasm after EGK.VI-VII. We also found similar expression pattern of CVH after EGK.VII. The diffused expression of DAZL in cytoplasm was thought to be the initiation of germline-specific transcription. Therefore, considering their mitotic feature with clustering in our results, we proposed that PGCs in chicken arise from at EGK.VI-VII which are derived from presumptive PGCs (pPGC) containing the germplasm localized in subcellular region based on the nomenclature of Nieuwkoop and Sutasurya (Nieuwkoop and Sutasurya, 1979). Also, the diffused expression of DAZL in cytoplasm was thought to be the initiation of germline-specific transcription. Germline-specific transcription during or after germ cell

specification is closely related with transcriptional repression in germ cells (Nakamura and Seydoux, 2008). Germline-specific transcription starts after specification in C. elegans (Seydoux and Fire, 1994) and Drosophila (Zalokar, 1976), while it is correlated with specification in mouse (Saitou et al., 2002). Thus, how germline competency is maintained during specification will be studied by investigation of transcriptional repression in germ cells in the further study. Conclusively, we reported that origin of PGCs and their dynamics during specification in chicken. Also, DAZL is a great maker to trace germ cells in chicken being expressed specifically in germ cells from cleavage stages to adult stages. DAZL seem to be one of germplasm components as well as CVH, and PGCs arise at least EGK.VI-VII with initiation of germline-specific transcription in chicken. After demonstration of origin of PGCs, we studied the potency of PGCs. *in vivo* manipulating PGCs in chicken is relatively easy via *in ovo* system compared to other species

To identify the potency of primordial germ cells after cytotoxic effect, we targeted embryonic stages. To eliminate endogenous PGCs in chickens by busulfan treatment, a sustained-release emulsion of busulfan using an SPG pumping connector was used in a previous study (Nakamura et al., 2010). Busulfan can specifically target and kill germ cells in embryonic gonads or testes leading to the depletion of endogenous germ cells. Also, PGCs which are a precursor of gametes may be a major target for the germ cell depletion and sterilization. Therefore, busulfan has been used to produce PGC-mediated germline chimeras by direct injection into blastoderm of fertilized eggs in chickens (Song et al., 2005; Nakamura et al., 2008; Nakamura et al., 2010). When injected into EG&K stage X, busulfan efficiently removed endogenous PGCs. To our knowledge, restoration of endogenous PGCs

after busulfan treatment has not been reported to date.

In both sexes, the relative PGC ratios of the busulfan-treated group to the normal embryos at 9 days were markedly higher than that those at day 5.5. Also, sexually mature male and female chickens treated with busulfan at stage X were able to produce functional sperms or eggs. These results indicated that germ cells were recovered from the cytotoxic effects of busulfan during development. Thus, we hypothesized the existence of a compensation mechanism to recover from busulfan toxicity in PGCs. To confirm the increase in PGCs after busulfan treatment, we conducted flow cytometry to enumerate the increase in PGC number. The number of PGCs in the busulfan-treatment group recovered to ~60% that of the control group. This suggested the existence of compensation and/or recovery mechanism in response to cytotoxic damage in PGCs, which is one of the characteristics of stem cells. A strong defensive mechanism against cytotoxic damage has been demonstrated in various stem cells, including SSCs and embryonic stem cells (Choi et al., 2004; Saretzki et al., 2008). To determine whether this compensation is caused by changes in the cell cycle, we conducted flow cytometry with PI staining to discriminate non-proliferating and proliferating PGCs after busulfan treatment. The decrease in the proportion of G0/G1 phase and increase that of S/G2/M phase PGCs after busulfan treatment indicated that the cell cycle status of some PGC populations changed from quiescent (G0) to proliferative (S/G2/M) phases.

Our data suggest that endogenous PGCs can recover from the cytotoxic effects of busulfan. The cell cycle status of PGCs shifted to a lower proportion in the G0/G1 phase and a higher proportion in the

S/G2/M phase after busulfan treatment, which indicates that the recovery of PGCs is strongly associated with the cell cycle transition. Our data increase our understanding of PGCs and provide an important basis for germ cell plantation studies.

Our next studies will be focused on the mechanism of action of germplasm-related genes during germ cell specification in chicken. Recently developed techniques of loss-of-function for genes by RNA interference are applicable to knock-down target genes. Furthermore, finding of novel function or genes that regulate PGC-potency will be one of major interests in the future. Taken together, our results in the present study will contribute to various research areas in life science.

REFERENCES

Anderson R, Copeland TK, Scholer H, Heasman J, Wylie C. 2000. The onset of germ cell migration in the mouse embryo. Mechanisms of Development 91:61-68.

Ando Y, Fujimoto T. 1983. Ultrastructural Evidence That Chick Primordial Germ-Cells Leave the Blood-Vascular System Prior to Migrating to the Gonadal Anlagen. Development Growth & Differentiation 25:345-352.

Ara T, Nakamura Y, Egawa T, Sugiyama T, Abe K, Kishimoto T, Matsui Y, Nagasawa T. 2003. Impaired colonization of the gonads by primordial germ cells in mice lacking a chemokine, stromal cell-derived factor-1 (SDF-1). Proc Natl Acad Sci U S A 100:5319-5323.

Bakst MR, Gupta SK, Akuffo V. 1997. Comparative development of the turkey and chicken embryo from cleavage through hypoblast formation. Poult Sci 76:83-90.

Bellairs R, Lorenz FW, Dunlap T. 1978. Cleavage in the chick embryo. J Embryol Exp Morphol 43:55-69.

Birkhead TR, Sheldon BC, Fletcher F. 1994. A comparative study of sperm-egg interactions in birds. J Reprod Fertil 101:353-361.

Bishop JB, Wassom JS. 1986. Toxicological review of busulfan (Myleran).

Mutat Res 168:15-45.

Bounoure L. 1939. L'origine des cellules reproductrices et le problème de la lignée germinale. Paris,: Gauthier-Villars. xii, 271 p. pp.

Bramwell RK, Marks HL, Howarth B. 1995. Quantitative determination of spermatozoa penetration of the perivitelline layer of the hen's ovum as assessed on oviposited eggs. Poult Sci 74:1875-1883.

Braude P, Pelham H, Flach G, Lobatto R. 1979. Post-transcriptional control in the early mouse embryo. Nature 282:102-105.

Buggia I, Locatelli F, Regazzi MB, Zecca M. 1994. Busulfan. Ann Pharmacother 28:1055-1062.

Callebaut M. 2005. Origin, fate, and function of the components of the avian germ disc region and early blastoderm: role of ooplasmic determinants. Dev Dyn 233:1194-1216.

Campion SN, Sandrof MA, Yamasaki H, Boekelheide K. 2010. Suppression of radiation-induced testicular germ cell apoptosis by 2,5-hexanedione pretreatment. III. Candidate gene analysis identifies a role for fas in the attenuation of X-ray-induced apoptosis. Toxicol Sci 117:466-474.

Chambers I, Silva J, Colby D, Nichols J, Nijmeijer B, Robertson M, Vrana J, Jones K, Grotewold L, Smith A. 2007. Nanog safeguards pluripotency and mediates germline development. Nature 450:1230-

U1238.

Chapman SC, Collignon J, Schoenwolf GC, Lumsden A. 2001. Improved method for chick whole-embryo culture using a filter paper carrier. Dev Dyn 220:284-289.

Cheng L, Gearing DP, White LS, Compton DL, Schooley K, Donovan PJ. 1994. Role of leukemia inhibitory factor and its receptor in mouse primordial germ cell growth. Development 120:3145-3153.

Choi JW, Kim S, Kim TM, Kim YM, Seo HW, Park TS, Jeong JW, Song G, Han JY. 2010. Basic fibroblast growth factor activates MEK/ERK cell signaling pathway and stimulates the proliferation of chicken primordial germ cells. PLoS One 5:e12968.

Choi YJ, Ok DW, Kwon DN, Chung JI, Kim HC, Yeo SM, Kim T, Seo HG, Kim JH. 2004. Murine male germ cell apoptosis induced by busulfan treatment correlates with loss of c-kit-expression in a Fas/FasL- and p53-independent manner. FEBS Lett 575:41-51.

Cook MS, Coveney D, Batchvarov I, Nadeau JH, Capel B. 2009. BAX-mediated cell death affects early germ cell loss and incidence of testicular teratomas in Dnd1(Ter/Ter) mice. Dev Biol 328:377-383.

Cooke JE, Heasman J, Wylie CC. 1996. The role of interleukin-4 in the regulation of mouse primordial germ cell numbers. Dev Biol 174:14-21.

De Felici M, Dolci S. 1991. Leukemia inhibitory factor sustains the survival of mouse primordial germ cells cultured on TM4 feeder layers. Dev Biol 147:281-284.

Deppe U, Schierenberg E, Cole T, Krieg C, Schmitt D, Yoder B, Vonehrenstein G. 1978. Cell Lineages of Embryo of Nematode Caenorhabditis-Elegans. Proc Natl Acad Sci U S A 75:376-380.

Down JD, Ploemacher RE. 1993. Transient and permanent engraftment potential of murine hematopoietic stem cell subsets: differential effects of host conditioning with gamma radiation and cytotoxic drugs. Exp Hematol 21:913-921.

Eberhart CG, Maines JZ, Wasserman SA. 1996. Meiotic cell cycle requirement for a fly homologue of human Deleted in Azoospermia. Nature 381:783-785.

Edgar BA, Datar SA. 1996. Zygotic degradation of two maternal Cdc25 mRNAs terminates Drosophila's early cell cycle program. Genes Dev 10:1966-1977.

Ephrussi A, Lehmann R. 1992. Induction of Germ-Cell Formation by Oskar. Nature 358:387-392.

Everett NB. 1945. The Present Status of the Germ-Cell Problem in Vertebrates. Biological Reviews of the Cambridge Philosophical Society 20:45-55.

Extavour CG, Akam M. 2003. Mechanisms of germ cell specification across the metazoans: epigenesis and preformation. Development 130:5869-5884.

Eyal-Giladi H, Ginsburg M, Farbarov A. 1981. Avian primordial germ cells are of epiblastic origin. J Embryol Exp Morphol 65:139-147.

Eyal-Giladi H, Kochav S. 1976. From cleavage to primitive streak formation: a complementary normal table and a new look at the first stages of the development of the chick. I. General morphology. Dev Biol 49:321-337.

Fabian B, Eyal-Giladi H. 1981. A SEM study of cell shedding during the formation of the area pellucida in the chick embryo. J Embryol Exp Morphol 64:11-22.

Fofanova KA. 1965. Morphologic Data on Polyspermy in Chickens. Fed Proc Transl Suppl 24:239-247.

Forrest KM, Gavis ER. 2003. Live imaging of endogenous RNA reveals a diffusion and entrapment mechanism for nanos mRNA localization in Drosophila. Current Biology 13:1159-1168.

Fujiwara Y, Komiya T, Kawabata H, Sato M, Fujimoto H, Furusawa M, Noce T. 1994. Isolation of a Dead-Family Protein Gene That Encodes a Murine Homolog of Drosophila-Vasa and Its Specific Expression in Germ-Cell Lineage. Proc Natl Acad Sci U S A 91:12258-12262.

Ghosh D, Seydoux G. 2008. Inhibition of transcription by the Caenorhabditis elegans germline protein PIE-1: genetic evidence for distinct mechanisms targeting initiation and elongation. Genetics 178:235-243.

Ginsburg M, Eyal-Giladi H. 1986. Temporal and spatial aspects of the gradual migration of primordial germ cells from the epiblast into the germinal crescent in the avian embryo. J Embryol Exp Morphol 95:53-71.

Ginsburg M, Eyal-Giladi H. 1987. Primordial germ cells of the young chick blastoderm originate from the central zone of the area pellucida irrespective of the embryo-forming process. Development 101:209-219.

Ginsburg M, Hochman J, Eyal-Giladi H. 1989. Immunohistochemical analysis of the segregation process of the quail germ cell lineage. Int J Dev Biol 33:389-395.

Guan K, Nayernia K, Maier LS, Wagner S, Dressel R, Lee JH, Nolte J, Wolf F, Li MY, Engel W, Hasenfuss G. 2006. Pluripotency of spermatogonial stem cells from adult mouse testis. Nature 440:1199-1203.

Guan K, Wagner S, Unsold B, Maier LS, Kaiser D, Hemmerlein B, Nayernia K, Engel W, Hasenfuss G. 2007. Generation of functional cardiomyocytes from adult mouse spermatogonial stem cells. Circ Res 100:1615-1625.

Hamburger V, Hamilton HL. 1951. A Series of Normal Stages in the

Development of the Chick Embryo. J Morphol 88:49-&.

Han JY. 2009. Germ cells and transgenesis in chickens. Comp Immunol Microbiol Infect Dis 32:61-80.

Hanyu-Nakamura K, Sonobe-Nojima H, Tanigawa A, Lasko P, Nakamura A. 2008. Drosophila Pgc protein inhibits P-TEFb recruitment to chromatin in primordial germ cells. Nature 451:730-733.

Haston KM, Tung JY, Reijo Pera RA. 2009. Dazl functions in maintenance of pluripotency and genetic and epigenetic programs of differentiation in mouse primordial germ cells in vivo and in vitro. PLoS One 4:e5654.

Hay B, Jan LY, Jan YN. 1988. A Protein-Component of Drosophila Polar Granules Is Encoded by Vasa and Has Extensive Sequence Similarity to Atp-Dependent Helicases. Cell 55:577-587.

Hayashi K, Lopes SMCD, Kaneda M, Tang FC, Hajkova P, Lao KQ, O'Carroll D, Das PP, Tarakhovsky A, Miska EA, Surani MA. 2008. MicroRNA Biogenesis Is Required for Mouse Primordial Germ Cell Development and Spermatogenesis. PLoS One 3.

Heasman J, Quarmby J, Wylie CC. 1984. The mitochondrial cloud of Xenopus oocytes: the source of germinal granule material. Dev Biol 105:458-469.

Heys F. 1931. The problem of the origin of germ cells. Quarterly Review of Biology 6:1-45.

Hird SN, Paulsen JE, Strome S. 1996. Segregation of germ granules in living Caenorhabditis elegans embryos: Cell-type-specific mechanisms for cytoplasmic localisation. Development 122:1303-1312.

Houston DW, King ML. 2000. Germ plasm and molecular determinants of germ cell fate. Current Topics in Developmental Biology, Vol 50 50:155-181.

Ikenishi K, Kotani M, Tanabe K. 1974. Ultrastructural Changes Associated with Uv Irradiation in Germinal Plasm of Xenopus-Laevis. Dev Biol 36:155-168.

Illmense.K, Mahowald AP. 1974. Transplantation of Posterior Polar Plasm in Drosophila - Induction of Germ-Cells at Anterior Pole of Egg. Proc Natl Acad Sci U S A 71:1016-1020.

Illmensee K, Mahowald AP. 1976. Autonomous Function of Germ Plasm in a Somatic Region of Drosophila Egg. Exp Cell Res 97:127-140.

Iwamoto T, Hiraku Y, Oikawa S, Mizutani H, Kojima M, Kawanishi S. 2004. DNA intrastrand cross-link at the 5'-GA-3' sequence formed by busulfan and its role in the cytotoxic effect. Cancer Sci 95:454-458.

Johnson AD, Bachvarova RF, Drum M, Masi T. 2001. Expression of axolotl DAZL RNA, a marker of germ plasm: widespread maternal RNA and onset of expression in germ cells approaching the gonad. Dev Biol 234:402-415.

Kanatsu-Shinohara M, Inoue K, Lee J, Yoshimoto M, Ogonuki N, Miki H, Baba S, Kato T, Kazuki Y, Toyokuni S, Toyoshima M, Niwa O, Oshimura M, Heike T, Nakahata T, Ishino F, Ogura A, Shinohara T. 2004. Generation of pluripotent stem cells from neonatal mouse testis. Cell 119:1001-1012.

Karagenc L, Cinnamon Y, Ginsburg M, Petitte JN. 1996. Origin of primordial germ cells in the prestreak chick embryo. Dev Genet 19:290-301.

Kawase E, Hashimoto K, Pedersen RA. 2004. Autocrine and paracrine mechanisms regulating primordial germ cell proliferation. Mol Reprod Dev 68:5-16.

Kawase E, Yamamoto H, Hashimoto K, Nakatsuji N. 1994. Tumor necrosis factor-alpha (TNF-alpha) stimulates proliferation of mouse primordial germ cells in culture. Dev Biol 161:91-95.

Kehler J, Tolkunova E, Koschorz B, Pesce M, Gentile L, Boiani M, Lomeli H, Nagy A, McLaughlin KJ, Scholer HR, Tomilin A. 2004. Oct4 is required for primordial germ cell survival. Embo Reports 5:1078-1083.

Kerr CL, Hill CM, Blumenthal PD, Gearhart JD. 2008. Expression of pluripotent stem cell markers in the human fetal ovary. Hum Reprod 23:589-599.

Kloc M, Bilinski S, Chan AP, Etkin LD. 2001. Mitochondrial ribosomal RNA in the germinal granules in Xenopus embryos revisited.

Differentiation 67:80-83.

Knaut H, Pelegri F, Bohmann K, Schwarz H, Nusslein-Volhard C. 2000. Zebrafish vasa RNA but not its protein is a component of the germ plasm and segregates asymmetrically prior to germ-line specification. Dev Biol 222:224-224.

Kochav S, Ginsburg M, Eyal-Giladi H. 1980. From cleavage to primitive streak formation: a complementary normal table and a new look at the first stages of the development of the chick. II. Microscopic anatomy and cell population dynamics. Dev Biol 79:296-308.

Kosaka K, Kawakami K, Sakamoto H, Inoue K. 2007. Spatiotemporal localization of germ plasm RNAs during zebrafish oogenesis. Mechanisms of Development 124:279-289.

Kurimoto K, Yamaji M, Seki Y, Saitou M. 2008. Specification of the germ cell lineage in mice: a process orchestrated by the PR-domain proteins, Blimp1 and Prdm14. Cell Cycle 7:3514-3518.

Labosky PA, Barlow DP, Hogan BL. 1994. Mouse embryonic germ (EG) cell lines: transmission through the germline and differences in the methylation imprint of insulin-like growth factor 2 receptor (Igf2r) gene compared with embryonic stem (ES) cell lines. Development 120:3197-3204.

Lassalle B, Bastos H, Louis JP, Riou L, Testart J, Dutrillaux B, Fouchet P, Allemand I. 2004. 'Side Population' cells in adult mouse testis express

Bcrp1 gene and are enriched in spermatogonia and germinal stem cells. Development 131:479-487.

Lawson KA, Dunn NR, Roelen BA, Zeinstra LM, Davis AM, Wright CV, Korving JP, Hogan BL. 1999. Bmp4 is required for the generation of primordial germ cells in the mouse embryo. Genes Dev 13:424-436.

Lee SI, Lee BR, Hwang YS, Lee HC, Rengaraj D, Song G, Park TS, Han JY. 2011. MicroRNA-mediated posttranscriptional regulation is required for maintaining undifferentiated properties of blastoderm and primordial germ cells in chickens. Proc Natl Acad Sci U S A 108:10426-10431.

Lee YM, Jung JG, Kim JN, Park TS, Kim TM, Shin SS, Kang DK, Lim JM, Han JY. 2006. A testis-mediated germline chimera production based on transfer of chicken testicular cells directly into heterologous testes. Biol Reprod 75:380-386.

Macdonald J, Glover JD, Taylor L, Sang HM, McGrew MJ. 2010. Characterisation and Germline Transmission of Cultured Avian Primordial Germ Cells. PLoS One 5.

Mahowald AP. 2001. Assembly of the Drosophila germ plasm. International Review of Cytology - a Survey of Cell Biology, Vol 203 203:187-213.

Matsui Y, Tokitake Y. 2009. Primordial germ cells contain subpopulations that have greater ability to develop into pluripotential stem cells. Dev Growth Differ 51:657-667.

Matsui Y, Zsebo K, Hogan BLM. 1992. Derivation of Pluripotential Embryonic Stem-Cells from Murine Primordial Germ-Cells in Culture. Cell 70:841-847.

Mccoshen JA, Mccallion DJ. 1975. Study of Primordial Germ-Cells during Their Migratory Phase in Steel Mutant Mice. Experientia 31:589-590.

Medeiros LA, Dennis LM, Gill ME, Houbaviy H, Markoulaki S, Fu D, White AC, Kirak O, Sharp PA, Page DC, Jaenisch R. 2011. Mir-290-295 deficiency in mice results in partially penetrant embryonic lethality and germ cell defects. Proc Natl Acad Sci U S A 108:14163-14168.

Megosh HB, Cox DN, Campbell C, Lin HF. 2006. The role of PIWI and the miRNA machinery in Drosophila germline determination. Current Biology 16:1884-1894.

Mello CC, Schubert C, Draper B, Zhang W, Lobel R, Priess JR. 1996. The PIE-1 protein and germline specification in C. elegans embryos. Nature 382:710-712.

Meyer DB. 1964. The Migration of Primordial Germ Cells in the Chick Embryo. Dev Biol 10:154-190.

Mintz B, Russell ES. 1957. Gene-Induced Embryological Modifications of Primordial Germ Cells in the Mouse. Journal of Experimental Zoology 134:207-237.

Naito M, Sano A, Matsubara Y, Harumi T, Tagami T, Sakurai M, Kuwana T.

2001. Localization of primordial germ cells or their precursors in stage X blastoderm of chickens and their ability to differentiate into functional gametes in opposite-sex recipient gonads. Reproduction 121:547-552.

Nakamura A, Seydoux G. 2008. Less is more: specification of the germline by transcriptional repression. Development 135:3817-3827.

Nakamura Y, Usui F, Ono T, Takeda K, Nirasawa K, Kagami H, Tagami T. 2010. Germline replacement by transfer of primordial germ cells into partially sterilized embryos in the chicken. Biol Reprod 83:130-137.

Nakamura Y, Yamamoto Y, Usui F, Atsumi Y, Ito Y, Ono T, Takeda K, Nirasawa K, Kagami H, Tagami T. 2008. Increased proportion of donor primordial germ cells in chimeric gonads by sterilisation of recipient embryos using busulfan sustained-release emulsion in chickens. Reprod Fertil Dev 20:900-907.

Newport J, Kirschner M. 1982. A Major Developmental Transition in Early Xenopus-Embryos .2. Control of the Onset of Transcription. Cell 30:687-696.

Nieuwkoop PD, Suminski EH. 1959. Does the so called "germinal cytoplasm" play an important role in the development of the primordial germ cells? Arch Anat Microsc Morphol Exp 48(Suppl):189-198.

Nieuwkoop PD, Sutasurya LA. 1979. Primordial germ cells in the chordates : embryogenesis and phylogenesis. Cambridge Eng. ; New York:

Cambridge University Press. xi, 187 p. pp.

Noce T, Okamoto-Ito S, Tsunekawa N. 2001. Vasa homolog genes in mammalian germ cell development. Cell Structure and Function 26:131-136.

Ohinata Y, Ohta H, Shigeta M, Yamanaka K, Wakayama T, Saitou M. 2009. A Signaling Principle for the Specification of the Germ Cell Lineage in Mice. Cell 137:571-584.

Okamura D, Kimura T, Nakano T, Matsui Y. 2003. Cadherin-mediated cell interaction regulates germ cell determination in mice. Development 130:6423-6430.

Okamura D, Tokitake Y, Niwa H, Matsui Y. 2008. Requirement of Oct3/4 function for germ cell specification. Dev Biol 317:576-584.

Olsen MW. 1942. Maturation, fertilization, and early cleavage in the hen's egg. J Morphol 70:513-533.

Pannett CA, Compton A. 1924. The cultivation of tissues in saline embryonic juice. Lancet 1:381-384.

Park HJ, Park TS, Kim TM, Kim JN, Shin SS, Lim JM, Han JY. 2006. Establishment of an in vitro culture system for chicken preblastodermal cells. Mol Reprod Dev 73:452-461.

Park KJ, Kang SJ, Kim TM, Lee YM, Lee HC, Song G, Han JY. 2010.

Gamma-irradiation depletes endogenous germ cells and increases donor cell distribution in chimeric chickens. In Vitro Cellular & Developmental Biology-Animal 46:828-833.

Park TS, Han JY. 2000. Derivation and characterization of pluripotent embryonic germ cells in chicken. Mol Reprod Dev 56:475-482.

Park TS, Hong YH, Kwon SC, Lim JM, Han JY. 2003. Birth of germline chimeras by transfer of chicken embryonic germ (EG) cells into recipient embryos. Mol Reprod Dev 65:389-395.

Patterson JT. 1910. Studies on the early development of the hen's egg I History of the early cleavage and of the accessory cleavage. J Morphol 21:101-134.

Perry MM. 1987. Nuclear events from fertilisation to the early cleavage stages in the domestic fowl (Gallus domesticus). J Anat 150:99-109.

Pesce M, Farrace MG, Piacentini M, Dolci S, Defelici M. 1993. Stem-Cell Factor and Leukemia Inhibitory Factor Promote Primordial Germ-Cell Survival by Suppressing Programmed Cell-Death (Apoptosis). Development 118:1089-1094.

Pesce M, Klinger FG, De Felici M. 2002. Derivation in culture of primordial germ cells from cells of the mouse epiblast: phenotypic induction and growth control by Bmp4 signalling. Mech Dev 112:15-24.

Plusa B, Hadjantonakis AK, Gray D, Piotrowska-Nitsche K, Jedrusik A,

Papaioannou VE, Glover DM, Zernicka-Goetz M. 2005. The first cleavage of the mouse zygote predicts the blastocyst axis. Nature 434:391-395.

Probin V, Wang Y, Zhou D. 2007. Busulfan-induced senescence is dependent on ROS production upstream of the MAPK pathway. Free Radic Biol Med 42:1858-1865.

Raz E. 2003. Primordial germ-cell development: the zebrafish perspective. Nat Rev Genet 4:690-700.

Rengaraj D, Zheng YH, Kang KS, Park KJ, Lee BR, Lee SI, Choi JW, Han JY. 2010. Conserved expression pattern of chicken DAZL in primordial germ cells and germ-line cells. Theriogenology 74:765-776.

Resnick JL, Bixler LS, Cheng L, Donovan PJ. 1992a. Long-term proliferation of mouse primordial germ cells in culture. Nature 359:550-551.

Resnick JL, Bixler LS, Cheng LZ, Donovan PJ. 1992b. Long-Term Proliferation of Mouse Primordial Germ-Cells in Culture. Nature 359:550-551.

Reynolds N, Collier B, Maratou K, Bingham V, Speed RM, Taggart M, Semple CA, Gray NK, Cooke HJ. 2005. Dazl binds in vivo to specific transcripts and can regulate the pre-meiotic translation of Mvh in germ cells. Hum Mol Genet 14:3899-3909.

Richardson BE, Lehmann R. 2010. Mechanisms guiding primordial germ cell migration: strategies from different organisms. Nat Rev Mol Cell Biol 11:37-49.

Runyan C, Schaible K, Molyneaux K, Wang Z, Levin L, Wylie C. 2006. Steel factor controls midline cell death of primordial germ cells and is essential for their normal proliferation and migration. Development 133:4861-4869.

Saitou M, Barton SC, Surani MA. 2002. A molecular programme for the specification of germ cell fate in mice. Nature 418:293-300.

Saitou M, Yamaji M. 2010. Germ cell specification in mice: signaling, transcription regulation, and epigenetic consequences. Reproduction 139:931-942.

Sakurai T, Iguchi T, Moriwaki K, Noguchi M. 1995. The Ter Mutation First Causes Primordial Germ-Cell Deficiency in Ter/Ter Mouse Embryos at 8 Days of Gestation. Development Growth & Differentiation 37:293-302.

Saretzki G, Walter T, Atkinson S, Passos JF, Bareth B, Keith WN, Stewart R, Hoare S, Stojkovic M, Armstrong L, von Zglinicki T, Lako M. 2008. Downregulation of multiple stress defense mechanisms during differentiation of human embryonic stem cells. Stem Cells 26:455-464.

Saunders PT, Turner JM, Ruggiu M, Taggart M, Burgoyne PS, Elliott D,

Cooke HJ. 2003. Absence of mDazl produces a final block on germ cell development at meiosis. Reproduction 126:589-597.

Scaldaferri ML, Fera S, Grisanti L, Sanchez M, Stefanini M, De Felici M, Vicini E. 2011. Identification of side population cells in mouse primordial germ cells and prenatal testis. Int J Dev Biol 55:209-214.

Seydoux G, Fire A. 1994. Soma-germline asymmetry in the distributions of embryonic RNAs in Caenorhabditis elegans. Development 120:2823-2834.

Shamblott MJ, Axelman J, Wang SP, Bugg EM, Littlefield JW, Donovan PJ, Blumenthal PD, Huggins GR, Gearhart JD. 1998. Derivation of pluripotent stem cells horn cultured human primordial germ cells. Proc Natl Acad Sci U S A 95:13726-13731.

Smith LD. 1966. Role of a Germinal Plasm in Formation of Primordial Germ Cells in Rana Pipiens. Dev Biol 14:330-&.

Snook RR, Hosken DJ, Karr TL. 2011. The biology and evolution of polyspermy: insights from cellular and functional studies of sperm and centrosomal behavior in the fertilized egg. Reproduction 142:779-792.

Song Y, D'Costa S, Pardue SL, Petitte JN. 2005. Production of germline chimeric chickens following the administration of a busulfan emulsion. Mol Reprod Dev 70:438-444.

Stern CD. 1998. Detection of multiple gene products simultaneously by in situ hybridization and immunohistochemistry in whole mounts of avian embryos. Current Topics in Developmental Biology, Vol 50 36:223-243.

Stern CD. 2005. The chick; a great model system becomes even greater. Dev Cell 8:9-17.

Strome S, Wood WB. 1982. Immunofluorescence Visualization of Germ-Line-Specific Cytoplasmic Granules in Embryos, Larvae, and Adults of Caenorhabditis-Elegans. Proceedings of the National Academy of Sciences of the United States of America-Biological Sciences 79:1558-1562.

Subramaniam K, Seydoux G. 1999. nos-1 and nos-2, two genes related to Drosophila nanos, regulate primordial germ cell development and survival in Caenorhabditis elegans. Development 126:4861-4871.

Surani MA, Saitou M, Erhardt S, Western P. 2002. The origin and properties of the mouse germ cell lineage. Journal of Medical Genetics 39:S13-S13.

Suzuki H, Tsuda M, Kiso M, Saga Y. 2008. Nanos3 maintains the germ cell lineage in the mouse by suppressing both Bax-dependent and -independent apoptotic pathways. Dev Biol 318:133-142.

Swift CH. 1914. Origin and early history of the primordial germ-cells in the chick. Baltimore. 1 p.l., p. 483-516. illus. pp.

Tadros W, Lipshitz HD. 2009. The maternal-to-zygotic transition: a play in two acts. Development 136:3033-3042.

Tam PP, Zhou SX. 1996. The allocation of epiblast cells to ectodermal and germ-line lineages is influenced by the position of the cells in the gastrulating mouse embryo. Dev Biol 178:124-132.

Tanaka SS, Toyooka Y, Akasu R, Katoh-Fukui Y, Nakahara Y, Suzuki R, Yokoyama M, Noce T. 2000. The mouse homolog of Drosophila Vasa is required for the development of male germ cells. Genes Dev 14:841-853.

Technau GM, Camposortega JA. 1986. Lineage Analysis of Transplanted Individual Cells in Embryos of Drosophila-Melanogaster .3. Commitment and Proliferative Capabilities of Pole Cells and Midgut Progenitors. Rouxs Archives of Developmental Biology 195:489-498.

Toyooka Y, Tsunekawa N, Takahashi Y, Matsui Y, Satoh M, Noce T. 2000. Expression and intracellular localization of mouse Vasa-homologue protein during germ cell development. Mechanisms of Development 93:139-149.

Tsang TE, Khoo PL, Jamieson RV, Zhou SX, Ang SL, Behringer R, Tam PP. 2001. The allocation and differentiation of mouse primordial germ cells. Int J Dev Biol 45:549-555.

Tsuda M, Sasaoka Y, Kiso M, Abe K, Haraguchi S, Kobayashi S, Saga Y. 2003. Conserved role of nanos proteins in germ cell development.

Science 301:1239-1241.

Tsunekawa N, Naito M, Sakai Y, Nishida T, Noce T. 2000. Isolation of chicken vasa homolog gene and tracing the origin of primordial germ cells. Development 127:2741-2750.

Ukeshima A, Yoshinaga K, Fujimoto T. 1991. Scanning and transmission electron microscopic observations of chick primordial germ cells with special reference to the extravasation in their migration course. J Electron Microsc (Tokyo) 40:124-128.

Van Buul PP, De Rooij DG, Zandman IM, Grigorova M, Van Duyn-Goedhart A. 1995. X-ray-induced chromosomal aberrations and cell killing in somatic and germ cells of the scid mouse. Int J Radiat Biol 67:549-555.

Wang H, Dey SK. 2006. Roadmap to embryo implantation: clues from mouse models. Nat Rev Genet 7:185-199.

Weber S, Eckert D, Nettersheim D, Gillis AJM, Schafer S, Kuckenberg P, Ehlermann J, Werling U, Biermann K, Looijenga LHJ, Schorle H. 2010. Critical Function of AP-2gamma/TCFAP2C in Mouse Embryonic Germ Cell Maintenance. Biol Reprod 82:214-223.

Weinberger C, Penner PL, Brick I. 1984. Polyingression, an Important Morphogenetic Movement in Chick Gastrulation. American Zoologist 24:545-554.

Whitington PM, Dixon KE. 1975. Quantitative Studies of Germ Plasm and Germ-Cells during Early Embryogenesis of Xenopus-Laevis. J Embryol Exp Morphol 33:57-74.

Williamson A, Lehmann R. 1996. Germ cell development in Drosophila. Annual Review of Cell and Developmental Biology 12:365-391.

Wishart GJ. 1997. Quantitative aspects of sperm:egg interaction in chickens and turkeys. Anim Reprod Sci 48:81-92.

Xu EY, Moore FL, Pera RA. 2001. A gene family required for human germ cell development evolved from an ancient meiotic gene conserved in metazoans. Proc Natl Acad Sci U S A 98:7414-7419.

Yamaji M, Seki Y, Kurimoto K, Yabuta Y, Yuasa M, Shigeta M, Yamanaka K, Ohinata Y, Saitou M. 2008. Critical function of Prdm14 for the establishment of the germ cell lineage in mice. Nat Genet 40:1016-1022.

Yeom YI, Fuhrmann G, Ovitt CE, Brehm A, Ohbo K, Gross M, Hubner K, Scholer HR. 1996. Germline regulatory element of Oct-4 specific for the totipotent cycle of embryonal cells. Development 122:881-894.

Ying Y, Liu XM, Marble A, Lawson KA, Zhao GQ. 2000. Requirement of Bmp8b for the generation of primordial germ cells in the mouse. Mol Endocrinol 14:1053-1063.

Ying Y, Zhao GQ. 2001. Cooperation of endoderm-derived BMP2 and

extraembryonic ectoderm-derived BMP4 in primordial germ cell generation in the mouse. Dev Biol 232:484-492.

Yoon C, Kawakami K, Hopkins N. 1997. Zebrafish vasa homologue RNA is localized to the cleavage planes of 2- and 4-cell-stage embryos and is expressed in the primordial germ cells. Development 124:3157-3165.

Zalokar M. 1976. Autoradiographic study of protein and RNA formation during early development of Drosophila eggs. Dev Biol 49:425-437.

Zamir E, Kam Z, Yarden A. 1997. Transcription-dependent induction of G1 phase during the zebra fish midblastula transition. Mol Cell Biol 17:529-536.

Zernicka-Goetz M, Plusa B, Piotrowska-Nitsche K. 2005. The role of cleavage pattern in the emerging asymmetry of the mouse embryo. Mechanisms of Development 122:S17-S17.

Zernicka-Goetz MZ. 2005. Cleavage pattern and emerging asymmetry of the mouse embryo. Nature Reviews Molecular Cell Biology 6:919-928.

Zohni K, Zhang X, Tan SL, Chan P, Nagano MC. 2012. The efficiency of male fertility restoration is dependent on the recovery kinetics of spermatogonial stem cells after cytotoxic treatment with busulfan in mice. Hum Reprod 27:44-53.

SUMMARY IN KOREAN

생식세포는 여러 세대를 거쳐 유전물질을 전달할 수 있는 유일한 세포 집단이다. 생식세포의 기원과 특성에 대한 연구는 발생생물학 및 진화생물학 분야에서 중요한 관심분야 중 하나이다. 여러 생물 종 중 조류의 생식세포의 기원과 특성에 대한 연구는 명확하게 밝혀져 있지 않다. 특히, 초기 발생과정이 시작되고 생식세포가 기원하는 난할시기에 대한 연구가 부족한 실정이다. 뿐만 아니라 재생의학 분야에서 중요한 분야 중 하나인 원시생식세포의 복원 능력에 대한 이해가 아직 부족하다. 본 연구에서, 우리는 닭의 자궁 내 시기 동안 배아의 발달 과정을 분석하였고, 생식세포 특이적 유전자 발현 패턴 검증을 통해 생식세포의 기원에 대해 연구하였다. 또한 부설판 처리 후 원시생식선에서의 생식세포 복원 능력에 대해 조사하였다.

첫 번째 연구에선 닭의 초기 배아 발달 과정의 구체적인 분석을 위하여, 화이트 레그혼 암탉의 자궁으로부터 복부마사지법을 통하여 알을 채취하였고, 광학현미경, 형광현미경 및 시간 차 비디오를 촬영하였다. 포유류의 경우와 달리, 비대칭적인 세포분열 (난할)이 초기 발달 동안 지속적으로 관찰되었다. 처음 두 번의 분열은 동시적으로 일어났지만, 그 이후로부터 비동시적인 분열이 관찰되었고, 세포분열이 주로 일어나는 가운데 지역의 경우, 바깥 지역에 비해 세포크기가 점점 줄어들었다. 또한 많은 수의 정자가 관찰되었는데, 응축 정자핵의 경우, 난황막 아래, 세포질 및 난황에 존재한 반면, 비응축 정자핵의 경우 오직 난황에 존재하였다. 결과적으로 이 연구를 통해 우리는 포유류와 확연한 차이를 보이는 정자 역동성과 세포분열을 관찰하였으며, 다정자증의 위치 및 수에 대해서 증명하였다.

닭의 초기 발달에 관한 결과 및 정보를 바탕으로. 다음으로 우리는 닭에서 생식세포의 기원에 대해서 조사하였다. 생식세포의 기원을 추적하기 위해, 생식세포 특이적 유전자 중 하나인 DAZL 유전자의 발현을 초기 배아 발달 동안 조사하였다. 우리는 기존에 보고했던 후기 일령 및 성축에서의 결과와 함께, DAZL 전사체가 닭의 전체 발달 기간 동안 생식세포에서만 특이적으로 발현함을 확인하였다. 난자에서 수정체으로 변이하는 과정 동안, DAZL 전사체는 난자의 핵 주위 및 접합체의 수정체의 가운데 부분에 국한되어 발현하였다. 배아의 난할시기 동안 우리는 DAZL 전사체의 발현 역동성을 관찰하였다. DAZL 전사체는 초기 난할시기 (EGK.I−III) 동안에는 분할고랑에, 난할 진행시기 (EGK.IV−VI) 동안에는 추정 원시생식세포 (pPGCs; presumptive primordial germ cells)의 세포질에 과립형태로 존재하였고, 마지막으로 후기 난할시기 (EGK.VI−X) 동안에는 원시생식세포 (PGCs) 의 세포질에 분산된 형태로 발현하였다. 위의 결과는 닭의 원시생식세포가 최소 EGK.VI에서부터 나타남을 시사해준다. 뿐만 아니라, 우리는 난할시기 동안 원시생식세포가 배반엽 상층 뿐 아니라 배반엽 하층에서도 존재함을 확인하였다. 종합적으로, 위의 결과들은 닭의 생식세포질이 생식세포의 특성화 과정 동안 지속적으로 가운데 지역에 존재하며, EGK.VI−VII에 생식세포 특이적 전사와 함께 주변 체세포로부터 구별됨을 보여준다.

배아발달과정 동안 부설판과 같은 독성 화학물질 처리 후 원시생식세포의 세포 반응에 대한 것은 잘 알려져 있지 않다. 그래서 우리는 부설판 처리 후 생식세포의 제거, 복원 능력 및 세포 주기 상태에 대해 조사하였다. 부설판을 먼저 분산유화체계를 이용해 유화시킨 후, 배반엽 시기의 알의 난황에 주입하였다. 그 다음으로 우리는 유세포 분석기를 통해 원시생식세포 수의 변화를 측정하였고, 면역조직화학법을 통해 원시생식세포의 분열을 조사하였다.

결과적으로, 부설판 처리 후, 수컷과 암컷 각각의 9일령 및 7일령에서 5.5일령과 비교하였을 때, 원시생식세포의 수가 대조군에 비해 60% 정도 증가하였다. 이것은 부설판에 의한 세포 독성에 대한 원시생식세포의 회복 능력이 있음을 시사해준다. 세포주기 분석 결과, 암컷과 수컷 모두에서 9일령에 대조군에 비해 G0/G1 기의 원시생식세포수가 유의적으로 줄어들고, S/G2/M 기의 원시생식세포수가 유의적으로 증가했음을 확인하였다. 뿐만 아니라, 5−ethynyl−2−deoxyuridine (EdU) 도입을 통한 세포증식 분석 결과, 생식세포 특이적 마커인 VASA 양성 세포 중 EdU 양성 세포의 비율이 부설판 처리군에서 유의적으로 증가하였음을 관찰하였다. 위의 결과를 통해, 원시생식세포가 세포독성에 노출되면, 세포주기를 증진시켜 복원경로를 거친다는 것을 밝혔다.

위의 결과들을 볼 때, 닭의 초기 배아 발달과 난할 과정은 포유류의 것과 매우 다름을 알 수 있다. 난할 진행 과정에 대한 생물학적 메커니즘을 알기 위해선, 세포운명 및 배아축형성, 유전자 발현양상 및 기능적 연구가 수행되어야 할 것이다. 또한 다정자증의 생물학적 기능 연구는 조류의 특징적인 발생에 대한 이해를 도울 것이다. 조류의 생식세포는 미리 운명 지어진 형태로 생각된다. 그러나 이것을 명확히 하기 위해선, 생식세포 특성화와 관련한 신호전달경로가 존재하는지, 수정란 게놈 활성화 (ZGA; zygotic genome activation)가 언제 일어나는지에 대한 연구가 추가적으로 요구된다. 또한 추후 연구에선 부설판 처리 후 원시생식세포의 복원을 조절하는 기작을 밝혀야만 할 것이다. 결과적으로 본 연구에서 우리의 결과는 닭의 초기 배아, 생식세포 및 원시생식세포의 잠재능력에 대한 발달 역동성에 대한 이해를 높일 수 있을 것이다.